J. Membrane Biol. 80, 27–47 (1984)

The Journal of
Membrane Biology


# KCl Transport across an Insect Epithelium: II. Electrochemical Potentials and Electrophysiology

J.W. Hanrahan* and J.E. Phillips
Department of Zoology, University of British Columbia, Vancouver, British Columbia, Canada V6T 2A9

**Summary.** The cellular mechanism of K-stimulated Cl transport in locust hindgut was studied using double-barrelled ion-sensitive microelectrodes and electrophysiological techniques. Steady-state net electrochemical potentials for Cl and K and the conductances of apical and basal membranes and paracellular pathway were determined under control conditions, during exposure to 1 mM cAMP, and following ion substitutions. Under control open-circuit conditions, intracellular Cl activity ($a^c_{Cl}$) was 3.5 times that predicted for passive equilibrium across the apical membrane. The net electrochemical potential opposing Cl entry from the mucosal side ($\Delta\bar{\mu}^a_{Cl}/F$) increased by 50% during cAMP stimulation of transepithelial Cl absorption whereas the net electrochemical potential favoring Cl exit across the basal membrane ($-\Delta\bar{\mu}^b_{Cl}/F$) was unchanged. No correlation was observed between $\Delta\bar{\mu}^a_{Cl}/F$ and the net electrochemical potential across the apical membrane for Na. The net electrochemical potential favoring K entry across the apical membrane ($-\Delta\bar{\mu}^a_K/F$) was negligible under $I_{sc}$ conditions when Cl transport rate was approximately 10 $\mu$eq cm$^{-2}$ hr$^{-1}$. Locust rectal cells showed electrical and dye coupling. The results also indicate that most transepithelial diffusion of ions is transcellular and that epithelial tightness effectively increases during exposure to cAMP because $R_a$ and $R_b$ both decrease by ~80% while $R_j$ is unchanged. The cAMP-induced $\Delta R_b$ was abolished in Cl-free saline whereas $\Delta R_a$ was insensitive to Cl removal, but was blocked by removing K from the saline. Based on these findings, our model for Cl absorption in locust hindgut features i) an active entry step for Cl at the apical membrane which is stimulated by cAMP and by low levels of K on the mucosal side, but is not energized by $-\Delta\bar{\mu}^a_{Na}/F$ or $-\Delta\bar{\mu}^a_K/F$ and ii) a large cAMP-stimulated Cl conductance in the basal membrane and a similar cAMP-stimulated K conductance in the apical membrane. cAMP dose-response curves are similar for the stimulation of active Cl absorption and Cl-independent (i.e. K) conductance, indicating that cAMP exerts dual control over active Cl transport and counter-ion permeability.

**Key Words** insect Cl absorption · intracellular ion activity · K-stimulated Cl transport · NaCl cotransport · epithelial transport · electrophysiology

* *Present address:* Dept. of Physiology, Yale University School of Medicine, 333 Cedar St., New Haven, CT 06510.

## Introduction

Previous tracer flux experiments indicated that active chloride transport across the rectum of the desert locust *Schistocerca gregaria* occurs by a mechanism which differs from the Na- and $HCO_3$-coupled models established in vertebrate epithelia. In the present paper we investigate this novel mechanism of Cl absorption using double-barrelled ion-sensitive microelectrodes and electrophysiological methods. Specifically, we attempt to localize the active step for transrectal Cl transport, to determine whether K stimulates active Cl transport directly or indirectly through changes in membrane potential, and to examine whether active Cl absorption is driven by transmembrane electrochemical potentials for Na or K through coupled ion movements (i.e. "secondary" active transport). We then investigate permeability and its regulation by cAMP. The results suggest that entry of Cl into rectal cells from the mucosal side is active, electrogenic, stimulated directly by cAMP and also by mucosal K, but is not energized by Na or K gradients at the apical membrane. Our findings suggest that locust rectum is a tight epithelium having low transepithelial resistance. Some of these findings were reported in preliminary form [21–23].

## Materials and Methods

### The Preparation

Locust recta were dissected and mounted as flat sheets in a Plexiglas® perfusion chamber which permitted microelectrodes access to the mucosal surface and separate perfusion of mucosal and serosal sides [20]. The tissue and microelectrode were viewed through a glass window at the end of the chamber using a dissecting microscope (Zeiss, Jena, GDR) at 25 to 100× magnifi-

cation, and were illuminated from front and rear by fiber optics (Intralux, 150 H, Volpi AG, Urdorf, Switz.). Transepithelial potential ($V_t$) was measured as before except that calomel half-cells were replaced with Ag/AgCl wires. Microelectrodes were advanced manually at an angle of 30 to 40° to the plane of the epithelium using Leitz micromanipulators (Wetzlar, F.R.G.). The tissue was continuously perfused with saline by gravity-feed from well-gassed reservoirs at 22 ± 1°C.

The following modifications were made to the saline described in the preceding paper for microelectrode experiments requiring ion substitutions: i) N-methyl-D-glucamine was substituted for Na and gluconate for Cl because choline and methylsulfate are sensed by K and Cl liquid ion-exchangers, respectively; ii) all salines were $HCO_3$-free and were oxygenated with 100% $O_2$ in order to minimize $HCO_3$ interference during intracellular Cl measurements. We showed in the companion paper that Cl transport and transepithelial electrical properties are not affected by removal of external $CO_2$ and $HCO_3$. External pH was 7.2 to 7.4.

## Ion Activity Measurements

The potential difference between reference and ion-sensitive barrels of the double-barrelled microelectrode ($V_i$) was measured using a differential electrometer having high input impedance ($\sim 10^{15}$ Ω; FD223, WP Instruments, New Haven, Conn.). The potential difference between the reference barrel within the cell and external mucosal and serosal agar bridges ($V_a$ and $V_b$, respectively) were measured individually using high impedance operational amplifiers ($10^{12}$ Ω; 4253, Teledyne Philbrick, Dedham, Mass.). Transepithelial resistance ($R_t$) was calculated from the deflections in $V_t$ produced by transepithelial current pulses and served to indicate gross damage as well as tissue viability. Saline resistance was determined by focusing the microscope just below the epithelial surface, removing the tissue, and then repositioning the microelectrode in the plane of focus for measurement of the voltage deflections caused by current pulses. The deflections in "apparent" $V_a$ that were produced by passing current pulses through the chamber with no tissue present were identical to those obtained immediately before impalements. Constant current pulses (~1-sec duration, 0.3 Hz) were supplied by waveform/pulse generators (Type 160 Series, Tektronix, Beaverton, Ore.) and measured as the voltage drop across a series resistor. Tissues were short-circuited with compensation for series resistance as before. After filtering (−3 db at 3 Hz), $V_t$, $V_a$, $V_b$, $V_i$, $I_t$ were recorded simultaneously using a 6-channel pen recorder (Brush 260, Gould Inc., St. Louis, Mo.) or, when fewer parameters were required, on a 2-channel recorder (7402A, Hewlett Packard, San Diego, Calif.). Signals were also monitored using a storage oscilloscope (D15, Tektronix) and $V_t$ was always displayed digitally (616, Keithley Instr. Inc., Cleveland, Ohio).

The techniques used for constructing double-barrelled microelectrodes were similar to those of Fujimoto and coworkers [14, 15, 27]. Capillary glass (1.0 mm OD, Frederick Haer and Co., Brunswick, Maine) was cleaned for at least 2 hr in conc. $HNO_3$, thoroughly rinsed with distilled water, dried in an oven, and stored dust-free at 0% relative humidity. Two glass capillaries were heated, rotated one-half turn, and drawn to a final tip diameter of less than 1 μm. After back-filling the reference barrel with acetone (ACS, Eastman Kodak Co., Rochester, N.Y.) electrodes were dipped into a 0.1% solution vol/vol of Dow Corning 1107 silicone oil in acetone for approximately 10 sec to silanize the ion-sensitive barrel and then were cured on a hot plate at ~300°C for 15 min. The electrode shaft was reinforced with fast-drying epoxy, and a 2- to 4-mm column of liquid-ion exchange resin (K, Corning 477317; Cl, Orion 92-17102; Na, monensin in Corning 477317) was injected into the silanized barrel from a syringe through fine polyethylene tubing and coaxed to the tip using a cat whisker. Electrodes were back-filled with 0.5 M KCl (for K and Cl exchangers) or 0.49 M NaCl at pH 3.0 (for Na exchanger).

Microelectrodes were calibrated frequently during the course of experiments in electrolyte solutions encompassing the entire range of intra- and extracellular ion activities. In most experiments 5, 50, 120, 500 mM KCl (conc.) solutions were used for calibrating K and Cl electrodes except during perfusion with nominally K- or Cl-free solutions, when 1 mM KCl was also included. Sodium microelectrodes were calibrated in pure solutions containing 1, 10, 100, 120 mM NaCl and mixed solutions containing 10 mM NaCl and 110 mM KCl. Ion activities in calibrating solutions were calculated using the modified Debye-Hückel equation [39].

Plots of microelectrode electromotive force (mV) against the logarithm of the ion activity (mM) in pure solutions yielded the following slopes ($s$) and $r^2$ values ($\bar{x} \pm$ SE): Cl, $s$ = 57.77 ± 0.8709 mV, $r^2$ = 0.9950 ± 0.0013, 29 electrodes; K, $s$ = 52.44 ± 0.62 mV, $r^2$ = 0.9961 ± 0.0008, 26 electrodes; Na, $s$ = 54.08 ± 1.4 mV, $r^2$ = 0.9988 ± 0.0007, 11 electrodes. These values compare well with previous studies [11, 14, 15, 27, 38, 44, 47]. Response time of the ion-sensitive barrel was usually about 1 to 3 sec except for Na-sensitive electrodes which occasionally required 15 to 20 sec to reach a stable value. The resistance of the ion-sensitive electrodes ranged between $2 \times 10^9$ and $5 \times 10^{10}$ ohms.

Selectivity coefficients of Cl microelectrodes against gluconate and sulfate interference were ($K_{Cl,gluc}$) = 0.039 ± 0.006 and $K_{Cl,SO_4}$ = 0.1324 ± 0.0215 when determined by the separate solution method [20]. The anion signal observed during perfusion with nominally Cl-free saline (i.e. apparent Cl activity after gluconate + sulfate substitution) was 5.2 mM, as expected using the microelectrode selectivity coefficients. Perfusion of recta for 3 hr with Cl-free saline resulted in apparent intracellular Cl activities, $a^c_{Cl}$, of 4.84 ± 0.38. An identical apparent Cl activity has been reported in heart muscle after prolonged exposure to methylsulfonate saline in the absence of $HCO_3$ (4.8 ± 0.6, [2]). Measurement of true residual intracellular Cl was not attempted since there is no method having the required sensitivity. It is unlikely that intracellular $HCO_3$ ($K_{Cl,HCO_3}$ = 0.2 to 0.09) accounts for all of the apparent Cl activity since salines were $HCO_3$-free and vigorously stirred with 100% $O_2$. Under this unnatural condition, the cells may contain some residual Cl, and replacement ions ($SO_4$ and gluconate) in addition to the interfering anions which are normally present. Since the validity of subtracting the residual $a^c_{Cl}$ measured in nominally Cl-free saline is debatable when the identity of the intracellular anion is not known under normal conditions, we did not correct for this possible error. Regardless, since $a^c_{Cl}$ normally ranged between 30 and 60 mM (i.e. six- to 12-fold larger) such interference would not change any of the conclusions in this study.

Na interference was ignored during intracellular K measurements since i) K electrodes showed high selectivity over Na ($K_{K,Na} < 0.02$), ii) measured intracellular Na activities were low ($a^c_{Na}$ = 8.0 ± 0.4 mM, 125 cells in 11 recta under $I_{sc}$ conditions), and iii) intracellular K was reduced to approximately 1 mM after prolonged perfusion with K-free saline (Fig. 4). Results obtained with Na-sensitive microelectrodes required corrections for K in-

terference. Selectivity for Na over K in eleven electrodes was 11.2 ± 1.1. Therefore, $a^c_K$ was measured immediately before or after $a^c_{Na}$ on the same tissues under each experimental condition.

Successful impalements were characterized by i) abrupt monotonic deflections in voltage, ii) stable intracellular potentials which remained within ±1 mV, iii) constant voltage divider ratios, and iv) return to the original baseline potentials upon retraction of the microelectrodes. No evidence of impalement damage was obtained using double-barrelled as opposed to single-barrelled microelectrodes, probably due to the large size of the columnar cells (~15 × 100 μm) and extensive infolding of the cell membranes.

## Effects of Transepithelial Salt Gradients

To measure the effects of single salt gradients, solutions containing 200 mM NaCl, KCl, choline Cl or K-methylsulfate were mixed separately with a sucrose solution (400 mM) in order to give intermediate concentrations of each salt (2, 8, 40 and 120 mM). These solutions also contained the normal eleven amino acids. $V_t$ was measured during exposure of the tissue to transepithelial concentration gradients of various salts. After equilibrating in $HCO_3$-free saline for 3 hr, both sides were exposed to the full strength (200 mM) salt solutions described above and re-equilibrated for a further 30 min. The mucosal or serosal side was then rapidly rinsed with lower concentrations of the same saline, alternating with the 200 mM full-strength solutions (e.g. sequence: 200, 2, 200, 8, 200, 40, 200, 120, 200 or reverse). A vacuum pump was used to drain the chambers while fresh saline was injected by syringe. Solution changes were completed within 10 sec. Control experiments showed that neither $V_t$ nor $R_t$ were altered artifactually by the technique of changing solutions and $V_t$ returned to approximately the same value between each test solution. The average discrepancy before and after a test run was 0.32 ± 0.32 mV following mucosal substitutions and 0.34 ± 0.12 mV after serosal substitutions ($\bar{x}$ ± SE, $n$ = 214). Net liquid junction potentials were measured by replacing the rectum with a short 3 M KCl agar bridge and were small (i.e. −0.45 mV between 200 mM NaCl and 2 mM NaCl + sucrose). It is clear that correcting for such small errors would strengthen our conclusion that transepithelial permeability properties are asymmetrical because liquid junctions would be of similar magnitude when testing gradients in opposite directions, and would therefore tend to increase the symmetry of $V_t$ responses.

Responses were slower when solutions were changed on the serosal side than on the mucosal side, often requiring several minutes to reach a stable value when the largest gradients were tested. This delay is probably due to subepithelial diffusion barriers (secondary cells, and muscle tissue) and the unstirred layer associated with them; however, the possibility of some change in intracellular composition cannot be ruled out during these slow transients.

## Voltage Scanning

This technique was used to explore the surface of the epithelium for regions of high conductance [13, 28, 36]. Current (250 μA $cm^{-2}$) was passed transepithelially while the potential difference between a "scanning" microelectrode, which was moved over the tissue surface, and the mucosal 3 M KCl agar bridge was monitored in order to determine the uniformity of the electrical field. The voltage between scanning electrode and agar bridge was measured using a differential electrometer (FD 223, W.P. Instr., New Haven, Conn.). This signal was filtered, displayed on a storage oscilloscope, and recorded using a pen recorder.

## Intracellular Injection of Fluorescent Dye

The fluorescent dye Lucifer Yellow CH was injected intracellularly by iontophoresis. A 3- to 5-mm column of dye was placed into the tip of the single-barrelled microelectrode by immersing the blunt end of the electrode into a 5% solution of Lucifer Yellow CH in distilled water (~0.1 M). Electrode tips were less than 1 μm dia. and had resistance of 25 to 40 or 10 to 15 MΩ after bevelling in a stream of abrasive [32]. Hyperpolarizing current was passed through the microelectrode by a constant current source (M 701, W.P. Instr., Tektronix, Beaverton, Ore.). A switch allowed passage of direct current or pulses. Current was monitored continuously using a storage oscilloscope. A second electrometer was used to measure current flowing through the microelectrode during dye injection and this was displayed digitally. Continuous impalement during dye injections was ensured by switching to pulse mode and observing the membrane potential between pulses, and a standard bridge was occasionally used to inject current and measure membrane potential simultaneously through the same electrode. Two cells at least 1 mm apart, were each injected for 30 to 45 min with −5 and −50 nA. This protocol allowed dye from the first injection to continue diffusing as the second cell was being filled; however, this should not affect the results noticeably since the dye spreads within seconds by diffusion (~200 μm $sec^{-1}$ [45]) and then, in locust rectum cells, appears to react preferentially with the nuclei. For processing, recta were pinned onto thin wafers of polymerized Sylgard 184 (Dow Corning Corp., Midland, Mich.; 2.3 $cm^2$ with 0.2 $cm^2$ hole cut in the center) and fixed in 4% paraformaldehyde buffered with 0.1 M phosphate at pH 7.2. After at least 1 hr of fixation, recta were dehydrated in ethanol (50, 80, 100% for 5, 5, 10 min, respectively) and then cleared for 5 min in methyl salicylate. Fluorescent cells were observed in whole mounts with incident excitation at 125 or 500× magnification (Orthoplan, Leitz Wetzlar, FRG). Photomicrographs were taken using an automatic camera attachment (Orthomat W, Leitz Wetzlar) and 35 mm Kodak Ektachrome 160 (Tungsten) film. Externally applied Lucifer Yellow was not taken up into cells across the plasma membrane.

## Electrical Coupling and Flat-Sheet Cable Analysis

Cell-cell coupling and cable analysis were determined using two single-barrelled microelectrodes. Current pulses (200 nA, 0.3 Hz, 1-sec duration) were passed intracellularly through one microelectrode and the resulting voltage deflections were measured in other cells using the second microelectrode. The distance between electrodes was measured using a calibrated eyepiece micrometer. Hyperpolarizing currents were usually used although depolarizing pulses gave similar results. Voltage responses were displayed on a storage oscilloscope after filtering and were measurable when greater than 0.3 mV. The mucosal and serosal sides are effectively short-circuited with respect to intracellular current in these experiments since the total resistance of the epithelium is much less than the resistance of the basal membrane in

the region of current spread (<0.5% in locust rectum; for discussion *see* [13, 28]). The voltage spread adjacent to the site of current injection is described by the differential equation [12, 13, 28, 36, 40]:

$$\frac{d^2V}{dx^2} + \frac{1}{x}\frac{dV}{dx} - \frac{V}{\lambda^2} = 0 \tag{1}$$

where $V$ is the voltage deflection at some distance $x$, and $\lambda$ is the space constant defined as $\sqrt{R_z/R_x}$. $R_z$ is the effective input resistance (resistance to ground: $R_aR_b/(R_a + R_b)$) in $\Omega cm^2$ and $R_x$ is the resistance to current flow within the epithelial sheet in $k\Omega$. Under the condition $V \to 0$ at $x = \infty$, the solution of Eq. (1) is $V = AK_o(x/\lambda)$, where $K_o$ is the zero-order modified Bessel function, $A$ is an integration constant (mV), and $x$ is distance ($\mu$m). Deflections in apical membrane potential were measured as a function of distance and compared to a set of curves obtained by drawing the Bessel function at 14 values of $\lambda$ between 50 and 800 $\mu$m using published tables [33]. Data were then fitted by eye to give $A$ and $\lambda$ which were then used to calculate $R_z$ according to

$$R_z = 2\pi A\lambda^2/I_o \tag{2}$$

where $I_o$ is the current injected intracellularly ($\mu$A) and symbols are described as above. The ratio of apical-to-basal membrane resistances ($\alpha$) was calculated, after corrections for series resistance (*see above*), from the deflections in apical and basal membrane potentials produced by transepithelial current pulses ($I_t$ = 20 $\mu$A/0.196 $cm^2$, 0.3 Hz, 1-sec duration) as

$$\alpha = \Delta V_a/\Delta V_b = R_a/R_b. \tag{3}$$

Resistance of the lateral intercellular space should not cause a significant underestimate of $R_a/R_b$ in this tissue since $\Delta V_a/\Delta V_b \leq 2$ and since the ratio of apical membrane : paracellular resistance is less than 4 [7]. Transepithelial resistance was determined as

$$R_t = (\Delta V_a + \Delta V_b)/I_t \tag{4}$$

where $I_t$ is transepithelial current as described above. Apical membrane resistance ($R_a$), basal membrane resistance ($R_b$), and junctional resistance ($R_j$) were then determined using the standard equations:

$$R_a = (1 + \alpha)R_z \tag{5}$$

$$R_b = (1 + \alpha)R_z/\alpha \tag{6}$$

$$R_j = (R_tR_a + R_tR_b)/(R_a + R_b - R_t) \tag{7}$$

which follow from the "lumped" equivalent electrical circuit model usually applied to epithelial tissues.

### Mannitol Space

Since changes in ion activity during cAMP stimulation might result from alterations in cell volume rather than ionic fluxes, nonmannitol space of recta was measured in normal saline, with or without 1 mM cAMP. Tissues were placed in small vials of vigorously oxygenated saline containing $^3$H-mannitol. After 1-hr incubation, three 1-$\mu$l samples of saline were counted by liquid scintillation to estimate $^3$H activity. Recta were blotted on bibulous paper and wet weight was determined to within ±0.1 mg. After drying to constant weight in a dessicating oven at 60°C, tissues were digested in 1 N KOH overnight, neutralized with conc. $H_2SO_4$, and counted as before. The difference between wet and dry weights was used as an estimate of total tissue water, and intracellular volume was calculated as the difference between total tissue water and mannitol space, assuming that mannitol distributes homogeneously throughout the extracellular space, does not enter the cells, and does not adsorb on the tissue surface. Similar estimates of mannitol space were obtained after 1 or 1.5 hr, suggesting that 1 hr was adequate for mannitol distribution to reach a steady state. $^3$H-mannitol space could not be checked using $^{14}$C-inulin because the cuticular intima is virtually impermeable to this polysaccharide; however, we showed in the previous paper that mannitol is not metabolized by locust rectum.

### Calculations and Statistics

Calibration curves for ion-sensitive microelectrodes were determined by standard linear regression. Net electrochemical potentials were calculated as:

$$\Delta\tilde{\mu}_i/F = RT(\ln a_i^c - \ln a_i^{m,s}/F) + zV_{a,b} \tag{8}$$

where $a_i^c$ is the activity of ion "$i$" in the cell, $a_i^{m,s}$ is the activity of ion "$i$" in mucosal or serosal solution, $V_a$ and $V_b$ are apical or basal membrane potentials, respectively, and $z$, $F$, $R$ and $T$ have their usual meanings. "Uphill" net electrochemical potentials are given as positive values; favorable electrochemical potentials are negative. Statistical comparisons were made using standard paired or unpaired $t$-tests.

## Results

### Electrochemical Potentials

#### *Steady-State Measurements of Intracellular Chloride and Potassium Activities*

Figure 1 shows traces of $V_t$, $V_a$, $V_b$ and intracellular ion activity obtained during impalements with double-barrelled K- and Cl-sensitive microelectrodes. Values were usually stable and showed little variability between cells in any particular tissue. Deflections in apical, basal and transepithelial potentials due to applied current pulses are also shown. Transient deflections in $V_i$, the potential difference between Cl-sensitive and reference barrels of the microelectrode, are artifacts which result from their having different time constants. K-sensitive microelectrodes had resistances that were one order of magnitude lower than those of Na or Cl electrodes, and generally did not show these transient deflections. As in previous open-circuit flux experiments, $V_t$ was initially 25 to 40 mV (mucosal-side positive) and decayed to approximately 8 mV after 2 to 3 hr.

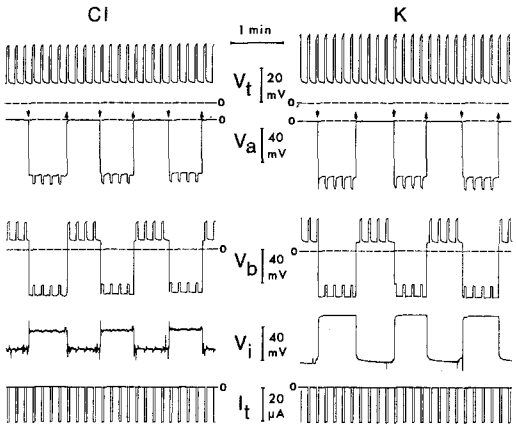


**Fig. 1.** Representative traces obtained using double-barrelled ion-sensitive microelectrodes. Simultaneous recording of transepithelial potential ($V_t$), apical membrane potential ($V_a$), basal membrane potential ($V_b$: also shows $V_t$ when the electrode is withdrawn into the mucosal half-chamber), potential difference between reference and ion-sensitive barrels of microelectrodes ($V_i$) under open-circuit conditions in normal saline. Transepithelial current pulses are shown at bottom ($I_t$)

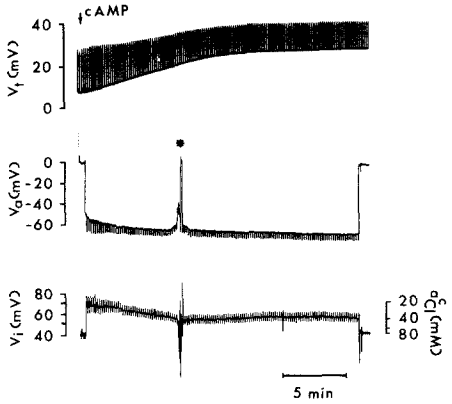


**Fig. 2.** Time-course of the effects of cAMP on $V_t$, $V_a$ and Cl-sensitive potential ($V_i$, differential). Deflections in $V_t$ and $V_a$ are due to transepithelial current pulses (20 μA/0.1962 cm²). The regular deflections in $V_i$ are artifacts which result from the difference between time constants of ion-sensitive and reference barrels. As indicated by $V_a$ and $V_i$, the electrode became dislodged after 8 min (at *) and a second cell was impaled

Control intracellular measurements were made when $V_t$ had declined to this level. Following addition of 1 mM cAMP or external K, approximately 30 min was required for the measured parameters to reach a new steady state. The time course of changes in $V_t$, $V_a$ and intracellular Cl activity is shown in Fig. 2. Steady-state measurements were made 30 to 60 min after switching to each new condition. Figure 3 shows impalement histograms of $a^c_{Cl}$ and $a^c_K$ measured in control preparations (unstimulated, 10 mM K), and during exposures to 1 mM cAMP and to K-free saline for 1 hr. Intracellular activities of Cl and K appear to be unimodal and seem reasonably normal in distribution about their mean values, suggesting that a single cell population was sampled and/or that there is effective cell-cell coupling.

*Chloride.* Table 1 summarizes the results of one series of experiments using double-barrelled Cl-sensitive microelectrodes. Under control (open-circuit) conditions, $a^c_{Cl}$ was 30.7 ± 1.1 mM, which is approximately 3.5-fold higher than predicted for passive distribution across the apical membrane (8 to 9 mM). There is a net Cl flux of ~4.5 μeq cm$^{-2}$hr$^{-1}$ to the serosal side ($J^{Cl}_{net}$) under these conditions; therefore, an active step must be postulated at the apical membrane while exit of Cl across the basal membrane may occur passively down a favorable electrochemical potential ($-\Delta\bar{\mu}^b_{Cl}$).

Serosal cAMP hyperpolarized $\Delta V_a$ by 6 mV and elevated $a^c_{Cl}$ by 16 mM. If a cAMP-stimulated Cl pump were located at the basal cell border, one would expect $a^c_{Cl}$ to either decrease or remain constant during cAMP exposure; an increase in $a^c_{Cl}$ is not consistent with stimulation of a pump in the basal membrane. When combined with the earlier finding that steady-state $J^{Cl}_{net}$ is elevated ~ ninefold under the same open-circuit conditions, these data indicate a cAMP-stimulated Cl pump at the apical membrane. It is interesting that $\Delta\bar{\mu}^b_{Cl}/F$ did not change significantly following cAMP addition although cAMP stimulates Cl flux through the membrane by ninefold. This finding hints that Cl conductance of the basal membrane might also be stimulated by cAMP if Cl exits by electrodiffusion, an idea that was confirmed using flat-sheet cable analysis (*see below*).

When external K was removed bilaterally in the presence of cAMP, $V_a$ hyperpolarized to ~−130 mV and then gradually declined, reaching −80 mV after 1 hr. $V_t$ increased temporarily and then declined to 4.8 ± 0.4 mV after 1 hr, consistent with the reduction in $J^{Cl}_{net}$ in K-free saline observed previously using tracers. Most importantly, $\Delta\mu^a_{Cl}/F$ declined in K-free saline, indicating that K stimulates active Cl entry. Note that if potassium stimulated $J^{Cl}_{net}$ by K depolarizing $V_a$ (thereby reducing the work needed for net Cl entry), then the uphill step required for Cl entry would have *increased* following K removal.

*Potassium.* Table 2 shows results obtained using double-barrelled K-sensitive microelectrodes under the same sequence of conditions as those just described for Cl. Values of $V_t$, $V_a$ and $V_b$ were simi-

lar to those obtained using Cl-sensitive microelectrodes (*compare* with Table 1). The mean intracellular K activity ($a^c_K$) was slightly below that predicted for equilibrium across the apical membrane; however, this difference was not significant ($P < 0.05$). Since $a^c_K$ would have to be above equilibrium across the apical membrane in order for $V_a$ to be attributed solely to a K-diffusion potential, some other electromotive force must be invoked at the apical membrane, such as an inward-directed, electrogenic Cl pump.

Small electrochemical potentials (<5 mV) favoring K absorption from mucosa-to-serosa were observed across the apical ($\Delta\bar{\mu}^a_K/F$) and basal ($\Delta\bar{\mu}^b_K/F$) membranes under control (unstimulated) conditions. This agrees with passive transepithelial K absorption, but alone does not exclude the presence of an additional small active flux. $^{42}K$ movements are largely passive in the absence of cAMP; i.e. there is no $J^K_{net}$ under these $I_{sc}$ conditions [19].

Serosal addition of cAMP dramatically increased $\Delta\bar{\mu}^a_K$ and $\Delta\bar{\mu}^b_K$, mostly because of changes in membrane potentials. Under open-circuit conditions, most of the large $J^K_{net}$ that is observed during tracer flux experiments [19, 23] can be explained by electrical coupling to active Cl absorption.

Locust rectal cells contained 14 mM K after perfusion with nominally K-free saline for 1 hr, and $a^c_K$ continued to decline to 1 mM over the next 2 hr (Fig. 4). Although the conditions were not strictly steady state with respect to $a^c_K$ after 1 hr, this does not influence our conclusions regarding the mode of

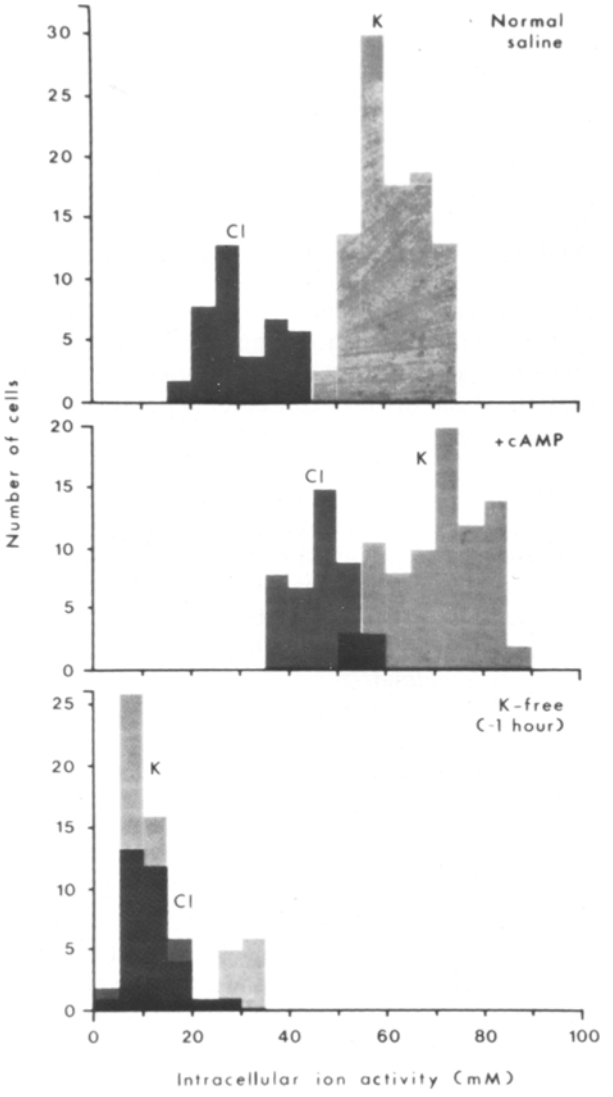


**Fig. 3.** Distribution of intracellular Cl and K activities in rectal pad epithelial cells under (open-circuit) control conditions, and after sequential exposure to 1 mM cAMP, and to K-free saline with cAMP present. $a^c_{Cl}$ and $a^c_K$ were measured in recta from different animals ($n$ = 6 to 10)

**Table 1.** Effects of adding cAMP and removing external K on electrical potentials, intracellular Cl activity, and calculated Cl electrochemical potentials[a]

| Sequential condition | $V_t$ (mV) | $V_a$ (mV) | $V_b$ (mV) | $a^c_{Cl}$ (mM) | $\Delta\bar{\mu}^a_{Cl}/F$ (mV) | $\Delta\bar{\mu}^b_{Cl}/F$ (mV) |
|---|---|---|---|---|---|---|
| Control (6; 40) | 8.6 ±0.3 | −57.0 ±0.8 | −48.7 ±0.9 | 30.7 ±1.1 | 32.0 ±1.2 | −23.3 ±1.4 |
| + 1 mM cAMP (6; 42) | 29.8 ±0.5 | −63.8 ±0.6 | −34.0 ±0.6 | 46.6 ±0.8 | 49.8 ±0.5 | −20.1 ±0.6 |
| + cAMP, K-free, after 1 hr (6; 42) | 4.8 ±0.4 | −79.6 ±4.8 | −74.8 ±5.0 | 11.8 ±0.9 | 28.3 ±4.2 | −23.5 ±4.4 |

[a] $V_t$, transepithelial potential; $V_a$, apical membrane potential; $V_b$, basal membrane potential; $a^c_{Cl}$ intracellular Cl activity; $\Delta\bar{\mu}^a_{Cl}/F$, $\Delta\bar{\mu}^b_{Cl}/F$, Cl net electrochemical potentials calculated for apical and basal membranes. Sign convention: $V_t$, mucosal side relative to serosal; $V_a$ and $V_b$, intracellular potential relative to mucosal and serosal side, respectively; $\Delta\bar{\mu}^a_{Cl}/F$ and $\Delta\bar{\mu}^b_{Cl}/F$, a positive sign indicates gradients opposing passive net Cl movement in the mucosal-to-serosal direction, negative sign indicates downhill gradients. Means ± SE, (number of recta; number of cells) for intracellular measurements; (number of recta; number of observations) for measurements of $V_t$ Extracellular [Cl] is 110 mM.

**Table 2.** Effects of adding cAMP and removing external K on electrical potentials, intracellular Cl activity, and calculated Cl electrochemical gradients

| Condition | $V_t$ (mV) | $V_a$ (mV) | $V_b$ (mV) | $a^c_K$ (mM) | $\Delta\bar{\mu}^a_K/F$ (mV) | $\Delta\bar{\mu}^b_K/F$ (mV) |
|---|---|---|---|---|---|---|
| Control (10; 97) | 7.2 ±0.3 | −57.8 ±0.5 | −50.7 ±0.3 | 61.4 ±0.7 | −3.3 ±0.5 | −3.9 ±0.3 |
| + 1 mM cAMP (9; 81) | 32.2 ±0.8 | −70.2 ±0.6 | −38.0 ±1.0 | 70.3 ±1.1 | −12.4 ±0.8 | −19.8 ±1.2 |
| + cAMP, K-free, after 1 hr (5; 58) | 9.8 ±0.7 | −84.1 ±3.4 | −74.3 ±3.3 | 13.9 ±1.2 | >55.2 ±2.0 | >−65.0 ±1.9 |

*See* footnote to Table 1 for explanations.

action of K on chloride transport because they are based on net $^{36}Cl$ fluxes and Cl electrochemical gradients when transepithelial transport is steady state. Moreover, as reported in the next section, similar results were obtained in experiments using recta more nearly depleted of K (<5 mM).

### *Effect of Bilateral K Additions on Cl and K Net Electrochemical Potentials under $I_{sc}$ Conditions*

Chloride-dependent $I_{sc}$ increases dramatically when K is added stepwise to both sides of K-depleted tissues [23]; however, from transepithelial measurements alone it was not clear whether this is an indirect electrical effect, for example membrane depolarization, a direct stimulation of the Cl pump, or both. A more direct action of K on Cl entry is indicated in the preceding section because removal of external K under open-circuit conditions reduces the net electrochemical potential opposing Cl entry, but to test this possibility further, electrical and chemical gradients for Cl across the apical and basal membranes were measured in short-circuited recta as a function of bilateral K concentration. This approach had the added advantage that $\Delta\bar{\mu}^a_{Cl}/F$ and $\Delta\bar{\mu}^a_K/F$ could be compared to find out whether Cl entry might be driven by K cotransport under $I_{sc}$ conditions, when the rate of active Cl transport is known.

Figure 5 illustrates intracellular potential ($V_i$), intracellular K and Cl activities, and calculated K and Cl electrochemical gradients. Data were obtained sequentially under the following conditions:

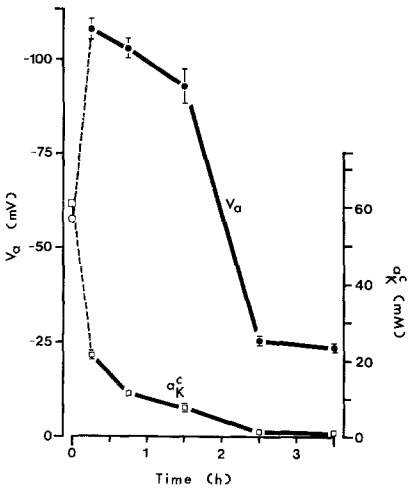


**Fig. 4.** Time-course of the decline in $a^c_K$ and $V_a$ during bilateral perfusion with K-free saline under open-circuit conditions. Each point is the mean ± SE of 6 measurements using a double-barrelled microelectrode in one tissue. Compare with $a^c_K$ = 61.4 ± 0.7 under control conditions

Unstimulated (K-free saline), cAMP-stimulated (K-free saline), cAMP-stimulated (with stepwise increases in potassium on both sides; [K] = 0, 2, 4, 10, 40, 100, 140 mM). Measurements were made at least 0.5 hr after exposure to cAMP and after each change in [K]: (i.e. steady-state conditions were approximated during all measurements). In nominally K-free saline, a $\Delta\bar{\mu}^a_K/F$ was estimated from the activity coefficient for K determined in normal saline (same ionic strength) and the level of K contamination measured using an atomic absorption spectrophotometer.

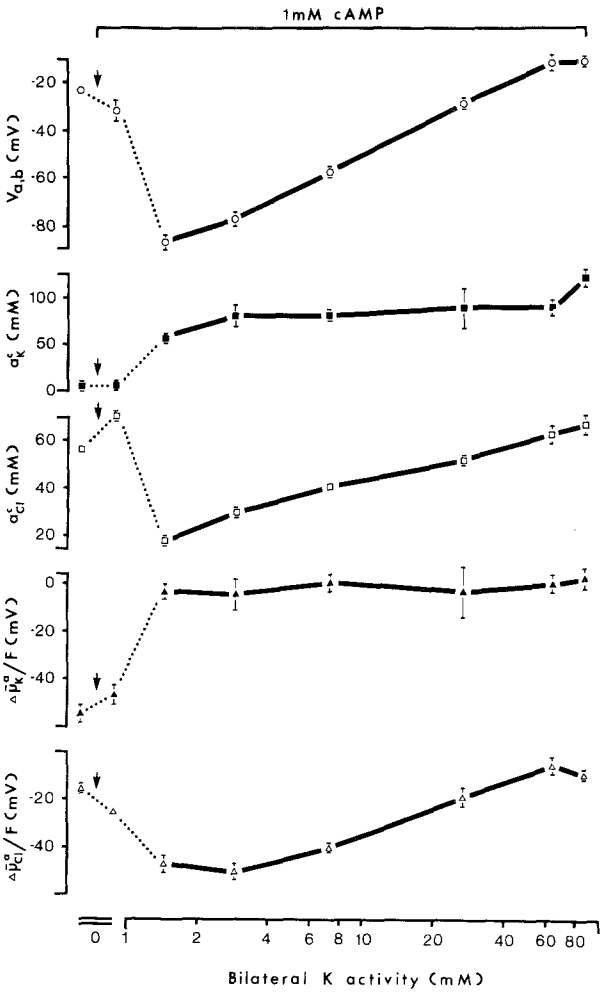


**Fig. 5.** Effects of 1 mM cAMP and then bilateral K additions on $V_i$, $a^c_K$, $a^c_{Cl}$, and calculated $\Delta\bar{\mu}^a_K/F$ and $\Delta\bar{\mu}^a_{Cl}/F$ (with respect to cytoplasm) under $I_{sc}$ conditions. Cyclic-AMP was added at the arrows during initial perfusion with nominally K-free saline. Note: i) $V_i$ changes about 50 mV/decade change in external K activity; ii) $a^c_K$ in K-depleted tissue increases from 3 mM to near control levels (65) when recta are re-exposed to 2 mM K; iii) $a^c_{Cl}$ decreases during hyperpolarization of $V_{a,b}$; iv) $\Delta\bar{\mu}^a_K/F$ is approximately 0 mV at all external K activities. Results shown are from one preparation; means ± SE; $n$ = 20 obs. ($V_i$), $n$ = 10 obs. ($a^c_K$, $a^c_{Cl}$, $\Delta\bar{\mu}^a_K/F$, $\Delta\bar{\mu}^a_{Cl}/F$)

Several points should be noted:

i) Exposing recta to K-free saline for more than 2.5 hr reduced $a^c_K$ to <5 mM (mean 1.6 mM) and depolarized both membranes to 23 mV.

ii) Serosal addition of 1 mM cAMP to K-depleted tissues increased $a^c_{Cl}$ by 12 mM, hyperpolarized $V_t$ by 15 mV (both changes significant at $P < 0.05$), and elevated the net electrochemical potential opposing Cl entry by 12 mV. All these observations are consistent with the previous tracer experiments that showed partial (35%) stimulation of Cl transport in the absence of external K and that the active step is at the apical membrane.

iii) Addition of K (2 or 4 mM) to both sides caused recovery of $a^c_K$ to control levels and membrane repolarization within 0.5 hr (*see* Fig. 6; external K activities of 1.44 and 2.89 mM, respectively). Under these $I_{sc}$ conditions, both $V_a$ and $V_b$ were virtually identical to the equilibrium potential ($E_K$). This is not surprising since the top panel shows that $V_a$ and $V_b$ vary approximately 50 mV per decade change in bilateral K activity.

iv) Adding K to both sides of the epithelium (0 to 4 mM) increased the electrochemical gradient opposing Cl entry ($\Delta\bar{\mu}^a_{Cl}/F$), consistent with previous observations under open-circuit conditions. Since $\Delta\bar{\mu}^a_{Cl}/F$ *increased* after K addition, the stimulation of active Cl transport by small amounts of K cannot be explained by simple depolarization of the apical membrane potential and a more direct stimulatory action of K on Cl entry must be postulated (*see* Discussion).

v) There is no correlation between $\Delta\bar{\mu}^a_K/F$ and $\Delta\bar{\mu}^a_{Cl}/F$ when external K is varied. In fact, $\Delta\bar{\mu}^a_K/F$ is not different from zero under $I_{sc}$ conditions over the range of 4 to 140 mM K ($P > 0.2$).

In summary, the results of varying bilateral [K] under $I_{sc}$ conditions indicate that $\Delta\bar{\mu}^a_K/F$ could not drive Cl entry because K is near electrochemical equilibrium across both membranes. Importantly, bilateral additions of K (2 to 4 mM) under $I_{sc}$ conditions elevate the unfavorable $\Delta\bar{\mu}^a_{Cl}/F$ across the apical membrane while increasing $J^{Cl}_{net}$, indicating that K enhances active Cl entry. Only at higher external concentrations of K would membrane depolarization enhance Cl absorption.

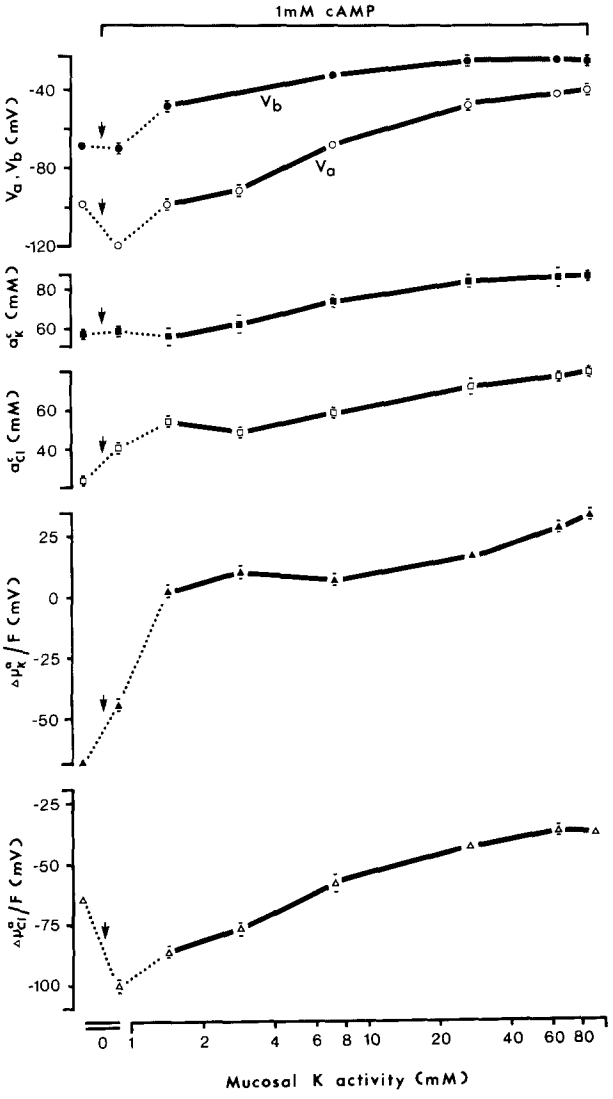


**Fig. 6.** Effects of sequential cAMP and mucosal K additions on $V_a$, $V_b$, $a^c_K$, $a^c_{Cl}$, and calculated $\Delta\bar{\mu}^a_K/F$ and $\Delta\bar{\mu}^a_{Cl}/F$ (with respect to cytoplasm) under open-circuit conditions during serosal perfusion with normal saline (10 mM K). Measurements were made 30 to 60 min after exposure to each condition. Note: i) $a^c_K$ during mucosal perfusion with nominally K-free is similar to that observed when mucosal [K] = 10 mM; ii) $\Delta\bar{\mu}^a_{Cl}$ declines progressively as mucosal [K] is elevated. Results from one preparation. Means ± SE; $n$ = 20 obs. ($V_a$, $V_b$), $n$ = 10 obs. ($a^c_K$, $a^c_{Cl}$, $\Delta\bar{\mu}^a_K/F$, $\Delta\bar{\mu}^a_{Cl}/F$)

### *Effects of Mucosal K Addition on Cl and K Electrochemical Potentials under Open-Circuit Conditions*

The mucosal side is normally positive with respect to the serosal side *in vivo* and [K] varies only in the lumen. To measure electrochemical potentials under these conditions, tissues were left open-circuited while [K] was increased from 0 to 140 mM on the mucosal side and serosal [K] was maintained at 10 mM (Fig. 6).

The following observations are noteworthy:

i) When mucosal K activity was 0 mM, addition of 1 mM cAMP to the serosal side hyperpolarized $V_a$ by 20 mV *and* increased $a^c_{Cl}$, consistent with stimulation of an electrogenic Cl pump in the apical membrane.

ii) $a^c_K$ is near control levels (≈60 mM) when the mucosal side is perfused with nominally K-free saline for >2.5 hr. Under these conditions intracellular K must have been acquired from the serosal side, presumably via a Na/K exchange pump in the basal membrane.

iii) Increasing mucosal [K] from 0 to 10 mM while maintaining 10 mM K on the serosal side depolarized $V_a$, in contrast to the preceding experiment in which $V_a$ and $\Delta\bar{\mu}^a_{Cl}$ both increased when [K] was raised bilaterally. Under open-circuit conditions, the stimulatory effect of mucosal K on the active entry step and $\Delta\bar{\mu}^a_{Cl}$ is probably obscured by a very large outward-directed K diffusion potential which results from the K gradient from cell (65 mM) to mucosal solution (nominally K-free).

### *Effects of Altering the Electrochemical Potential for Na across the Apical Membrane*

Previous results indicated that Cl transport across locust rectum is relatively insensitive to Na removal [23]. Nevertheless, even trace quantities of Na might sustain NaCl coentry in the presence of a favorable Na electrochemical gradient across the apical membrane ($\Delta\bar{\mu}^a_{Na}$) provided that the affinity of the carrier is exceptionally high and Na is recycled locally [16].

Figure 7 shows typical recordings of impalements made using double-barrelled Na-sensitive microelectrodes under $I_{sc}$ conditions when recta were perfused with normal saline bilaterally and 1 mM cAMP on the serosal side. The $a^c_{Na}$ averaged 8.01 ± 0.41 mM and intracellular potential was 58.06 ± 0.54 ($\bar{x}$ ± SE, 125 cells, 11 tissues). Large net electrochemical potentials favored Na entry across both cell membranes. $a^c_{Na}$ changed little when mucosal [Na] was reduced to 49 μM.

We examined the relationship between mucosal [Na] (measured using an atomic absorption spectrophotometer) and $\Delta\bar{\mu}^a_{Na}/F$ or $\Delta\bar{\mu}^a_{Cl}/F$ which were calculated by measuring intracellular $a^c_{Na}$, $a^c_{Cl}$ and $V_i$ using double-barrelled ion-sensitive microelectrodes under $I_{sc}$ conditions. Extracellular Cl activities observed immediately before impaling cells were used to calculate electrochemical potentials and this was also true for Na at all concentrations except that of nominally Na-free saline in which it was not possible to measure external $a_{Na}$ reliably with liquid ion-exchanger microelectrodes. In the latter case, an atomic absorption spectrophotometer was used to measure Na concentration which was then corrected for the activity coefficient measured in normal saline which had the same ionic strength. As shown in Fig. 8, the Na gradient varied directly with mucosal [Na], as would be expected if

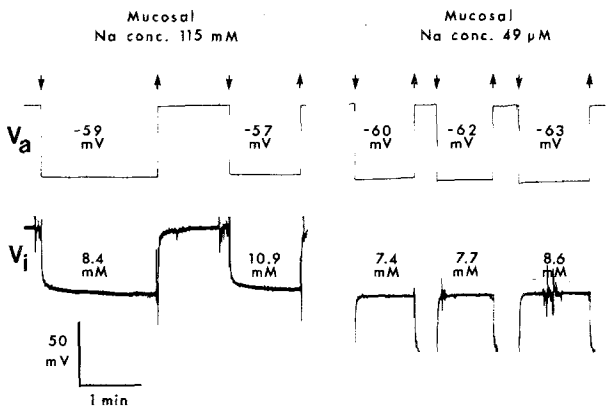


**Fig. 7.** Representative traces obtained during impalement of rectal tissue using a double-barrelled Na-sensitive microelectrode with $V_t$ clamped at 0 mV and mucosal perfusion with normal saline (115 mM Na) and then nominally Na-free saline (49 μM Na). The serosal side was bathed in normal saline throughout. Values of $V_a$ and $V_b$ were corrected for series resistance. $a^c_{Na}$ was corrected for electrode selectivity using K activities measured in the same tissue under both conditions. As shown at lower right, the differential Na-sensitive trace goes off-scale when the microelectrode is retracted into nominally Na-free saline (N-methyl-D-glucamine substituted)

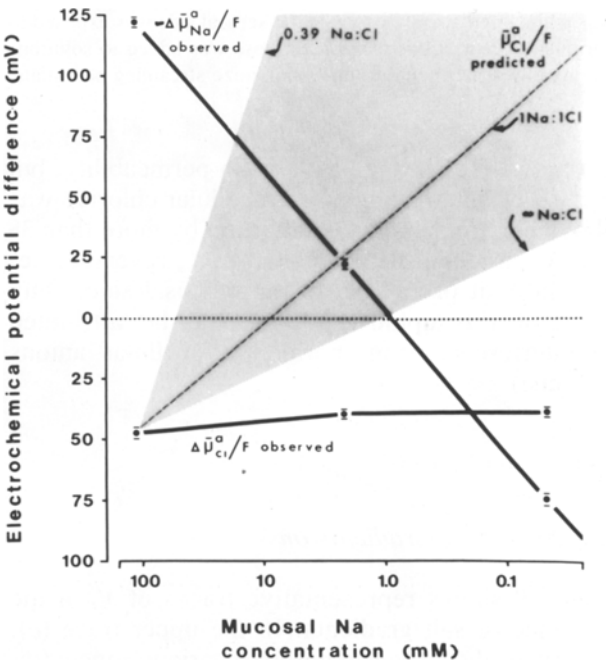


**Fig. 8.** Relationship between $-\Delta\bar{\mu}^a_{Na}/F$ and $\Delta\bar{\mu}^a_{Cl}/F$ in cAMP-stimulated recta with $V_t$ clamped at 0 mV. The calculated value of $-\Delta\bar{\mu}^a_{Na}/F$ declined linearly with slope ~58 mV/decade change in [Na] and reversed when mucosal [Na] was less than 1 mM. The shaded area shows energetically feasible trajectories for $\Delta\bar{\mu}^a_{Cl}/F$ if Cl were to enter across the apical membrane by "secondary" active transport driven by $\Delta\bar{\mu}^a_{Na}/F$. The dashed line shows the predicted values of $\Delta\bar{\mu}^a_{Cl}/F$ if Cl flux is coupled 1 : 1 with that of Na. Note that $\Delta\bar{\mu}^a_{Cl}/F$ falls completely outside the shaded region. Means ± SE; 58 to 125 impalements, 6 to 11 tissues

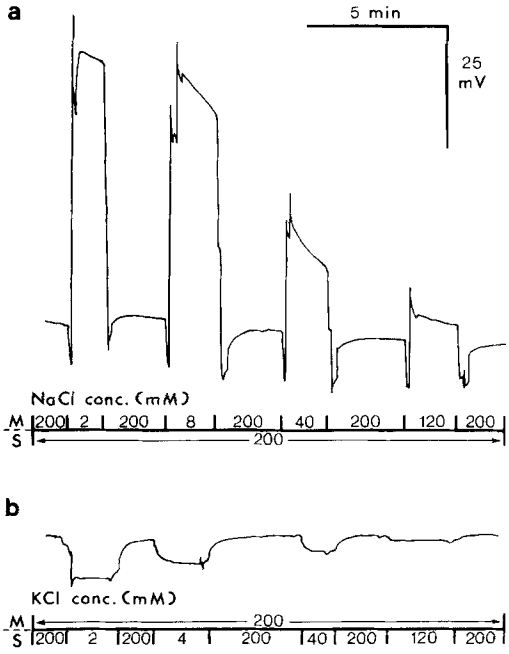


**Fig. 9.** Representative recordings of $V_t$ during exposure to transepithelial NaCl or KCl gradients. (*a*) Serosal (*S*) composition held constant (200 mM NaCl) and the mucosal side was exposed to solutions of increasing [NaCl] as indicated. (*b*) Mucosal [KCl] was maintained at 200 mM while the serosal side was exposed to various concentrations of KCl. Sucrose was added to solutions having low salt concentration to minimize streaming potentials

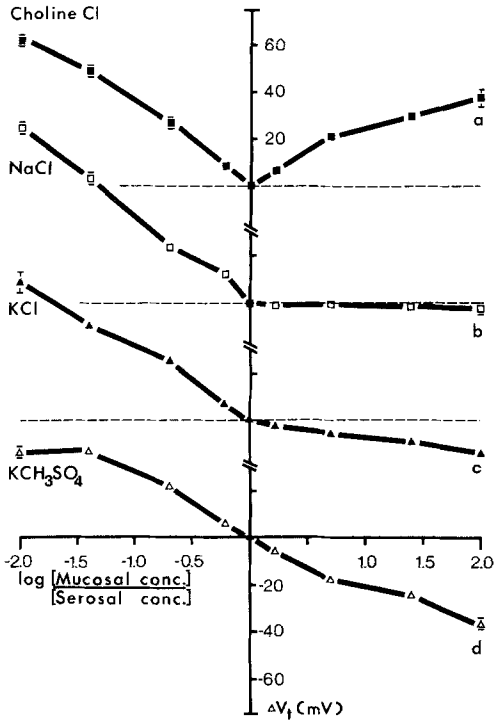


**Fig. 10.** Deflections in $V_t$ resulting from exposure of cAMP-stimulated recta to transepithelial salt gradients. (*a*) choline chloride, (*b*) sodium chloride, (*c*) potassium chloride, (*d*) potassium methylsulfate. Similar results were obtained using unstimulated or azide-poisoned tissues. Means ± SE; $n$ = 10 recta (NaCl), $n$ = 6 (KCl), $n$ = 8 (K-methylsulfate)

the apical membrane has low Na permeability, but $\Delta\bar{\mu}^a_{Cl}/F$ was not changed. Intracellular chloride was above electrochemical equilibrium by more than 38 mV, even when the calculated $\Delta\bar{\mu}^a_{Na}$ reversed; i.e. favored exit of cell Na to the mucosal side. Only 3.7% of this uphill $\Delta\bar{\mu}^a_{Cl}/F$ could be attributed to interference from normal intracellular anions (≈5 mM).

## Electrophysiology

### *Effects of Salt Gradients on $V_t$*

Figure 9 shows representative traces of $V_t$ in the presence of salt gradients. In the upper trace (*a*), the mucosal side was exposed to various concentrations of NaCl while serosal [NaCl] remained constant at 200 mM. When NaCl and KCl solutions were used, $V_t$ reached a maximum within a few seconds and then declined. Deflections in $V_t$ were less abrupt when solutions were changed on the serosal side and transients sometimes occurred at the serosal border but were not studied in detail. We considered $\Delta V_t$ during mucosal solution changes to be generally more accurate because they occurred instantly, so that there was little opportunity for changes in intracellular ion levels.

Figure 10 summarizes the relationship between the logarithm of the imposed gradient, and the change in $V_t$ produced across locust rectum by each salt solution. Transference numbers are not shown because they would be underestimated because of shunting by the paracellular pathway. Nevertheless, the effects of choline Cl, NaCl and KCl gradients are clearly asymmetrical, implying that transepithelial properties are determined by two barriers having different properties rather than by a single, symmetrical barrier as might be expected for the paracellular pathway. Also, the apical cell border, site of the active step for Cl transport, appears to be cation-selective and have low Cl permeability (Fig. 10).

### *Voltage Scanning*

No current leaks were observed when microelectrodes were moved over the epithelium proper, over the reduced epithelium between each rectal pad, or at the edge of the tissue where it was fastened to the chamber. Experimentally damaged ar-

**Fig. 11.** Fluorescence of rectal cells following injection of the central cell with Lucifer Yellow CH (50 nA for 30 min). The nuclei of 20 to 30 cells normally stain intensely after injecting dye into one cell

eas were easily located. We calculate that a 7.6 $\mu$m dia. hole would have been detectable assuming a voltage sensitivity between microelectrode and agar bridge of ~0.3 mV.

*Cell-Cell Coupling*

Figure 11 shows a typical result of Lucifer Yellow CH injection into one cell as observed by fluorescence microscopy. In recta from eleven locusts, eight out of thirteen experiments showed extensive diffusion of dye from injected into adjacent cells. The central cell was usually the brightest, and was presumed to be the one in which the microelectrode was situated. No preferential routes of coupling were observed; the stained area was circular and did not stain particular pathways or clusters of cells. Lucifer Yellow CH stained an average of 28 ± 4 cells and an area of 78.9 ± 13.8 $\mu m^2$ ($\bar{x}$ ± SE) after 30-min injections. Five out of 13 injected cells appeared to be uncoupled; however, four of these were within 200 $\mu$m of the edge of the rectal pads where the cuticular intima attaches to the rectum. It is possible that these cells were damaged and became uncoupled during dissection of the intima.

Figure 12 shows the effects of current injection into one cell on the apical membrane potential of a second cell located 42 $\mu$m from the point of injection. The *I/V* relation of intracellularly injected current measured in different cells was linear over the range of currents and in all salines used in this study. Coupling was also independent of the direction of current flow since voltage responses were identical when negative (hyperpolarizing) or positive (depolarizing) currents were injected, in contrast to many epithelia in which cells are uncoupled by depolarization [28, 41; reviewed in 29].

Finally, we tested whether large current pulses caused time-dependent uncoupling or deterioration of the membrane potential (this was important because membrane resistances were low, necessitating large pulses in order to measure the space constant). Depolarizing current pulses of 300 nA were injected into some rectal cells for 20 min with no

evidence of uncoupling or deterioration of membrane potential (data not shown).

### *Cell Membrane and Paracellular Resistance*

In order to estimate membrane resistances of locust rectum in the presence of cell-cell coupling, voltage deflections were measured at various distances from the point of current injection before and after addition of 1 mM cAMP as described in Materials and Methods (Fig. 13*a,b*). The best-fit Bessel functions are also shown as solid lines. Table 3 summarizes the results of cable analyses under control conditions, and during cAMP exposure in normal saline. The values of $R_a$, $R_b$ and $R_j$ suggest that the locust rectum is a tight epithelium, particularly during cAMP exposure when ~90 to 95% of passive ion movements across the tissue occur transcellularly. The resistances of locust rectum cell membranes after stimulation (30 to 40 $\Omega$ cm$^2$) are low compared to most other epithelia, but this is probably due to extensive membrane infolding which results in nine- to 200-fold amplification of membrane area. Addition of 1 mM cAMP caused a large decline in $R_t$ (65%) and reduced both apical and basal membrane resistances by about 80% (Table 3). The space constant ($\lambda$) declined from 420 to 219 $\mu$m ($P < 0.01$) after cAMP addition in normal saline. Junctional resistance was difficult to measure accurately in cAMP-treated tissues bathed in normal saline due to the low value of $R_z$, which declines as the square of $\lambda$. Nevertheless, no large changes in $R_j$ were observed under these conditions (Table 3) or in Cl-free saline when $R_z$ was higher during cAMP stimulation (Table 4).

Figure 14 shows that deflections in $V_a$ and $V_b$ produced by transepithelial current pulses were diminished after addition of 1 mM cAMP to the serosal side. To identify which ionic conductances were affected at each membrane, the effects of cAMP on $\Delta V_a$ and $\Delta V_b$ were measured during ion substitutions. In Cl-free saline (gluconate substituted), only the apical membrane resistance appeared to decrease during cAMP exposure (Fig. 15*a*) consistent with data shown in Table 4. In fact, $\Delta V_b$ actually increased under these conditions; however, this observation is not surprising because more current flows transcellularly when $R_a$ declines and this increase in current should cause larger deflections in the basal membrane potential even though $R_b$ remains constant. After prolonged perfusion of recta with KCl-free saline (Na gluconate substituted), cAMP had no effect on voltage deflections at either cell border, although polarization effects at the apical membrane made a valid cable analysis impossible under these conditions (Fig. 15*b*). These results suggest that the basal membrane contains a

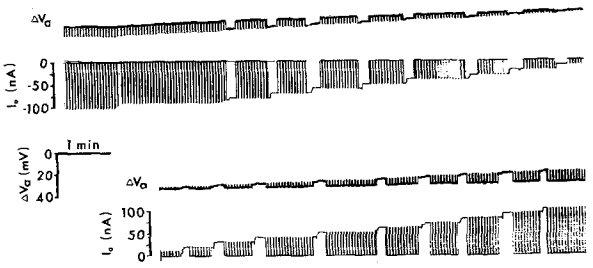


**Fig. 12.** Electrical coupling between cells in the rectal epithelium. Hyperpolarizing (upper traces) and depolarizing currents (lower traces) were passed from an adjustable constant-current source (10 to 100 nA, ~1-sec duration, square pulses) into a cell through one microelectrode, and the resulting deflections in apical membrane potential ($\Delta V_a$) were measured using a second microelectrode located 42 $\mu$m (~3 cells) from the point of current injection. Note that similar results were obtained with hyperpolarizing and depolarizing currents

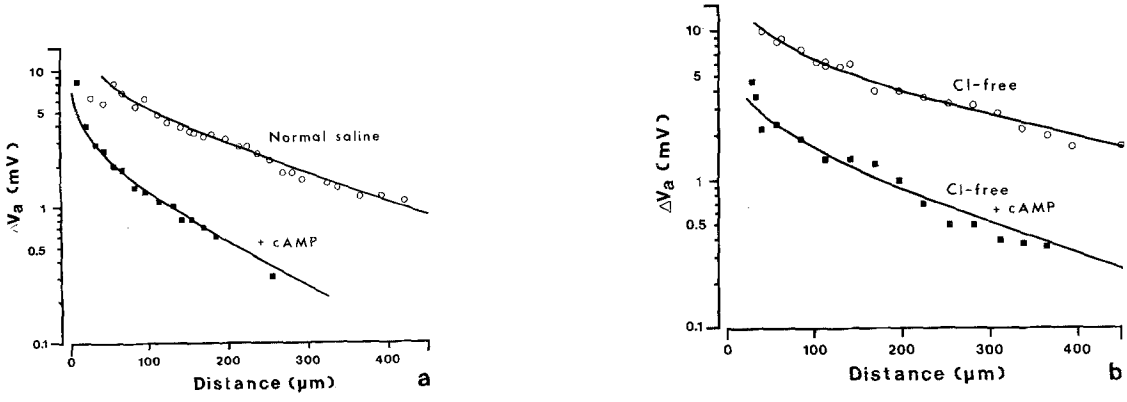


**Fig. 13.** Deflections in $V_a$ as a function of distance from the point of current injection before and after addition of cAMP in (*a*) Normal and (*b*) Cl-free saline. Measurements during cAMP exposure were made at least 30 min after addition of 1 mM cAMP to the serosal perfusate. The solid line indicates the best-fitting Bessel function obtained as described in the text

Cl-dependent conductance and the apical membrane contains a K-dependent conductance, both of which are stimulated by cAMP. Simultaneous stimulations of apical membrane K- and basal membrane Cl-conductances would explain why $\alpha$ remains constant during cAMP exposure while $R_t$ declines by 50 to 65%.

Table 4 shows the effects of cAMP on resistances under Cl-free conditions determined by cable analysis. As in normal saline, $R_a$ declined by 80% during cAMP exposure whereas basal membrane resistance was only slightly reduced. Basal membrane conductance ($G_b = 1/R_b$) increased by 22.6 mS cm$^{-2}$ in normal saline (114 mM Cl) as compared with only 0.4 mS cm$^{-2}$ in Cl-free saline.

*Effects of [cAMP] on $I_{sc}$ and $G_t$*

$I_{sc}$ and $G_t$ were measured as a function of [cAMP] for two reasons: First, if stimulations of $G_t$ and $I_{sc}$

**Table 3.** Electrical parameters estimated by cable analysis in normal saline

| Preparation | $R_t$ ($\Omega$ cm$^2$) | $\alpha$ | $R_z$ ($\Omega$ cm$^2$) | $R_x$ (k$\Omega$) | $A$ (mV) | $\lambda$ ($\mu$m) | $R_a$ ($\Omega$ cm$^2$) | $R_b$ ($\Omega$ cm$^2$) | $R_j$ ($\Omega$ cm$^2$) | Current direction | Number of cells |
|---|---|---|---|---|---|---|---|---|---|---|---|
| Control | | | | | | | | | | | |
| 1 | 213.9 | 0.80 | 70.0 | 34.6 | 1.10 | 450 | 126.0 | 184.6 | 687.0 | − | 14 |
| 2 | 280.4 | 0.91 | 90.3 | 44.6 | 1.42 | 400 | 183.3 | 178.0 | 1252.0 | − | 16 |
| 3 | 213.0 | 1.44 | 95.0 | 31.4 | 1.00 | 550 | 232.0 | 160.8 | 469.4 | − | 29 |
| 5a | 299.4 | 1.17 | 118.8 | 131.9 | 4.20 | 300 | 257.8 | 220.3 | 801.0 | + | 28 |
| 6a | 256.6 | 1.35 | 128.2 | 8.0 | 2.55 | 400 | 301.3 | 223.2 | 502.4 | + | 20 |
| 6b[a] | 256.6 | 1.35 | 115.6 | 7.2 | 2.30 | 400 | 271.7 | 201.3 | 560.9 | + | 21 |
| $\bar{x}$ ± SE | 252.7 | 1.13 | 100.5 | 50.3 | 2.05 | 420.0 | 220.1 | 193.4 | 742.4 | | |
| $n$ = 5 | ±17.4 | ±0.12 | ±10.4 | ±21.2 | ±0.60 | ±40.6 | ±30.3 | ±12.2 | ±141.1 | | |
| + 1 mM cAMP | | | | | | | | | | | |
| 4 | 63.7 | 2.05 | 17.6 | 44.0 | 1.4 | 200 | 53.7 | 26.2 | 314.2 | − | 26 |
| 5b[b] | 77.9 | 0.95 | 15.4 | 50.2 | 1.6 | 175 | 30.1 | 31.6 | 801.0 | + | 15 |
| 6c[b] | 82.7 | 0.67 | 12.6 | 31.4 | 1.0 | 200 | 21.1 | 31.3 | 560.9 | + | 15 |
| 7 | 109.3 | 1.30 | 31.1 | 34.6 | 1.10 | 300 | 71.5 | 55.0 | 803.9 | + | 22 |
| $\bar{x}$ ± SE | 76.7 | 1.24 | 19.2 | 40.1 | 1.27 | 218.8 | 44.1 | 36.0 | 559.1 | | |
| $n$ = 2,4 | ±15.0 | ±0.3 | ±4.1 | ±4.3 | ±0.14 | ±27.7 | ±11.4 | ±6.5 | ±244.9 | | |

[a] Cable analysis was repeated to test the reproducibility of the measurements.

[b] $R_z$ was extremely low during cAMP exposure (15.4, 12.6 $\Omega$ cm$^2$), approaching the limits of sensitivity of measurement. Since small errors resulted in nonsensical values of $R$, $R_a$ and $R_b$, it was necessary to calculate $R_a$ and $R_b$ in two recta from $R_t$ and $\alpha$ measured during cAMP stimulation and $R_j$ measured under control conditions, assuming that $R_j$ was not affected by cAMP. This assumption seems justified since no consistent effect of cAMP was observed in preparations in which $R_z$ was high enough to allow calculation of $R_j$ directly (*see also* Table 4).

**Table 4.** Results of cable analysis in Cl-free saline before and after adding 1 mM cAMP

| Preparation | $R_t$ ($\Omega$ cm$^2$) | $\alpha$ | $R_z$ ($\Omega$ cm$^2$) | $R_x$ (k$\Omega$) | $A$ (mV) | $\lambda$ ($\mu$m) | $R_a$ ($\Omega$ cm$^2$) | $R_b$ ($\Omega$ cm$^2$) | $R_j$ ($\Omega$ cm$^2$) | Current direction | Number of cells |
|---|---|---|---|---|---|---|---|---|---|---|---|
| Unstimulated | | | | | | | | | | | |
| 8 | 370.7 | 0.773 | 254.5 | 125.7 | 4 | 450 | 451.2 | 583.7 | 577.6 | + | 22 |
| 9a | 295.6 | 1.160 | 248.8 | 69.1 | 2.2 | 600 | 537.4 | 463.3 | 419.5 | − | 15 |
| 10a | 347.9 | 0.386 | 93.3 | 149.2 | 4.75 | 250 | 129.3 | 334.9 | 1388.6 | − | 17 |
| 11a | 390.7 | 0.473 | 159.3 | 150.8 | 4.8 | 325 | 234.6 | 496.0 | 839.8 | − | 17 |
| 12a | 438.7 | 0.222 | 138.2 | 86.4 | 2.75 | 400 | 168.6 | 759.5 | 832.0 | − | 12 |
| $\bar{x}$ ± SE | 368.7 | 0.603 | 178.8 | 116.2 | 3.70 | 405 | 304.2 | 527.5 | 811.5 | | |
| $n$ = 5 | ±23.6 | ±0.166 | ±31.4 | ±21.2 | ±0.60 | ±40.6 | ±30.3 | ±12.2 | ±141.1 | | |
| 1 mM cAMP added | | | | | | | | | | | |
| 8b | 210.1 | 0.111 | 33.3 | 44.0 | 1.4 | 275 | 37.0 | 333.3 | 485.7 | + | 17 |
| 9b | 231.0 | 0.286 | 127.2 | 62.8 | 2.0 | 450 | 163.6 | 572.0 | 336.7 | − | 21 |
| 10b | 243.3 | 0.118 | 25.4 | 113.1 | 3.6 | 150 | 28.4 | 240.7 | 2537.7 | − | 17 |
| 12b | 350.4 | 0.0631 | 33.9 | 84.8 | 2.7 | 200 | 36.0 | 571.2 | 828.4 | − | 9 |
| $\bar{x}$ ± SE | 258.7 | 0.145 | 55.0 | 74.2 | 2.43 | 268.8 | 66.3 | 429.3 | 1047.1 | | |
| $n$ = 2,4 | ±15.0 | ±0.3 | ±4.1 | ±4.3 | ±0.14 | ±27.7 | ±11.4 | ±6.5 | ±244.9 | | |

reflected two different processes, then $G_t$ and $I_{sc}$ might exhibit different cAMP dose-response curves. Second, a dose-response relationship for the Cl-independent effects of cAMP could be calculated by comparing the results obtained in normal and Cl-free saline.

Figure 16 shows the effects of [cAMP] on $G_t$ and $I_{sc}$ in normal and Cl-free saline. Both had "S"-shaped dose-response curves with similar threshold doses ($5 \times 10^{-5}$ M cAMP) and maximal responses at ~1 mM cAMP, suggesting that Cl-dependent and potassium conductances have similar cAMP sensitivities.

*Mannitol Space*

Although cAMP increases $a^c_{Cl}$ and $\Delta\bar{\mu}^a_{Cl}$, both these effects might be explained without postulating effects on a Cl pump if cAMP caused cell shrinkage. Intracellular volume was estimated as nonmannitol space in controls and during cAMP exposure as described in Materials and Methods. There was no significant change in $^3$H-mannitol space or cell volume between controls (3.61 ± 0.24 $\mu$l) and cAMP-treated tissues (3.79 ± 0.25 $\mu$l; $P > 0.2$), although the "nonmannitol space" declined drastically during exposure to hyperosmotic saline to 0.43 ± 0.11 $\mu$l.

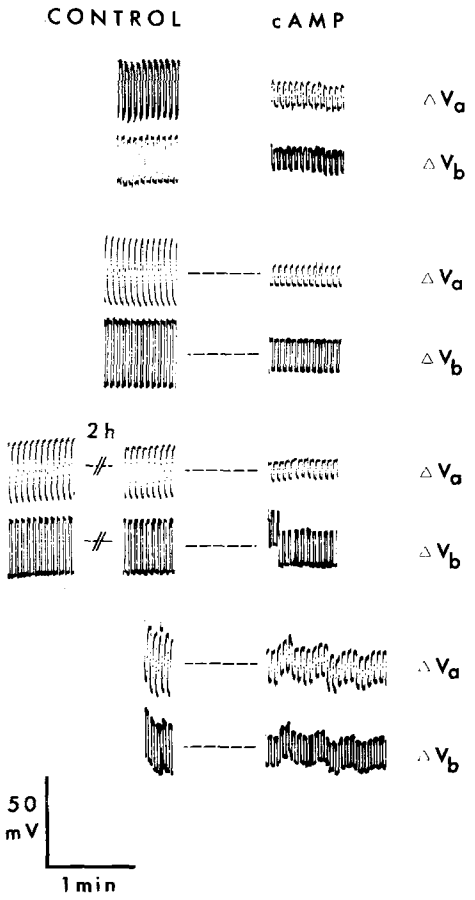


**Fig. 14.** Effects of cAMP on the deflections in apical and basal membrane potentials of recta produced by transepithelial current pulses (voltage divider ratio). Control conditions are shown at left. Results shown at right were obtained 30 to 60 min after adding cAMP to the serosal side. Voltage deflections were produced by transepithelial pulses of 20 $\mu$A/0.196 cm$^2$

## Discussion

Several observations confirm the viability of the preparation used in this study as well as the validity of microelectrode measurements. The salines and method of mounting tissues onto the chamber were identical to those used during previous tracer flux experiments. $V_t$ in the microelectrode chamber was initially high (25 to 40 mV, lumen positive) and declined exponentially to ~8 mV, identical to the values observed during previous tracer flux experiments where long-term viability of the tissue is well established. Moreover, short-circuit current was 250 to 300 $\mu$A cm$^{-2}$ after cAMP exposure during both microelectrode and flux studies. In the previous paper we found that $^{35}SO_4$ permeability is negligible when using this method of mounting tissues and suggested that edge damage is probably low. This suggestion is supported by the present electrophysiological data.

Membrane potentials and intracellular ion activities showed little variation within each preparation. Potential changes were abrupt after impalement, and potentials and ion activities remained constant during the course of measurements. Recordings were occasionally made from one cell for more than 30 min without detectable changes in membrane potentials, ion activity or voltage divider ratio. Also, no differences were observed between data from single- and double-barrelled microelectrodes although the latter are thought to cause impalement damage artifacts in some epithelia [10, 38].

No intracellular gradients were observed when microelectrodes were advanced deep into the epithelium. Also, only one electrical potential "well" was observed when electrodes were pushed through the tissue and only one population of cells was evident from the approximately normal distribution of intracellular ion activities. The underlying secondary cells do not constitute a continuous layer because they are penetrated by tracheoles, and thus probably do not contribute greatly to $R_t$.

## Measurements of Membrane Potentials and Intracellular Ion Activities

Membrane potentials observed in this study are "typical" for many vertebrate and invertebrate cells, and agree well with values for isolated recta of *Locusta migratoria* ($V_a$ = −65 to −59 mV, $V_b$ = −45 to −47 mV over the first 4 hr; [46]). Lower membrane potentials in *Schistocerca* recta were recorded by Phillips ([34]; $V_a$ = −50 mV, $V_b$ = −37 mV); however these early measurements were made *in situ* using microelectrodes with large tip diameters, thus the discrepancy might be due to the different experimental conditions used and/or to impalement damage.

Ion activities have not previously been measured in locust rectal cells; however, the results are similar to those observed in other epithelia. Somewhat higher $a_K^c$ (133 mM) and lower $a_{Cl}^c$ (9 to 10 mM) were reported in blowfly salivary gland, but in that preparation [3, 5], the luminal surface is bathed with KCl-rich fluid secreted by the gland rather than a "low-K" saline like the one used here. Reported values of $a_K^c$ in the "high PD" cells of lepidopteran midgut range from 75.7 mM [6] to 95 mM [31]. Finally, intracellular ion activities in the present study are in reasonable agreement with concentrations estimated chemically in homogenates of whole rectal tissue (55 mM Na, 88 mM K, 39 mM Cl; recta from water-fed locusts; [34]) and, except for lower Na, are in good agreement with electron microprobe data for cytoplasm of blowfly rectal papillae (23 to 47 mM Na, 65 to 85 mM K, 23 to 43 mM Cl; [18]).

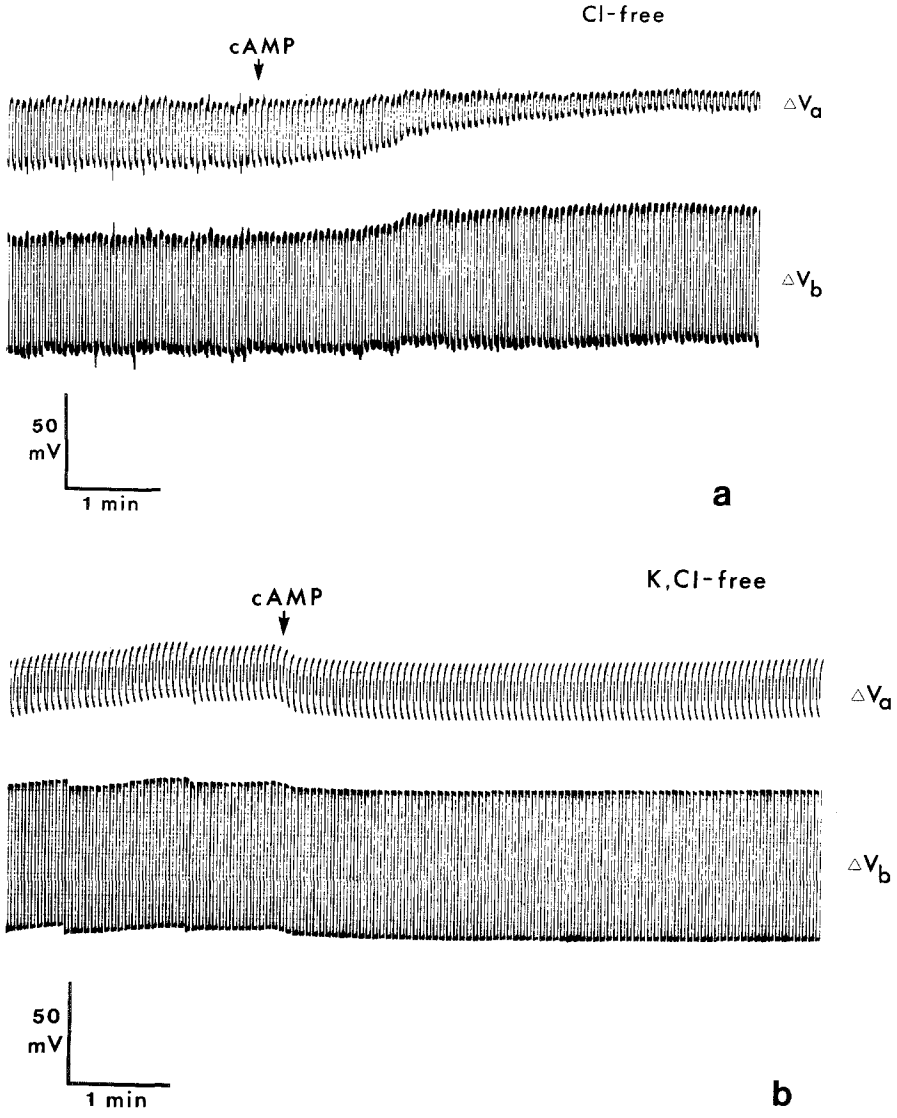


**Fig. 15.** (*a*) Effects of cAMP on the voltage divider ratio in Cl-free saline. Cyclic-AMP (1 mM) was added to the serosal side at the arrow. (*b*) Effects of cAMP on the voltage divider ratio under KCl-free conditions

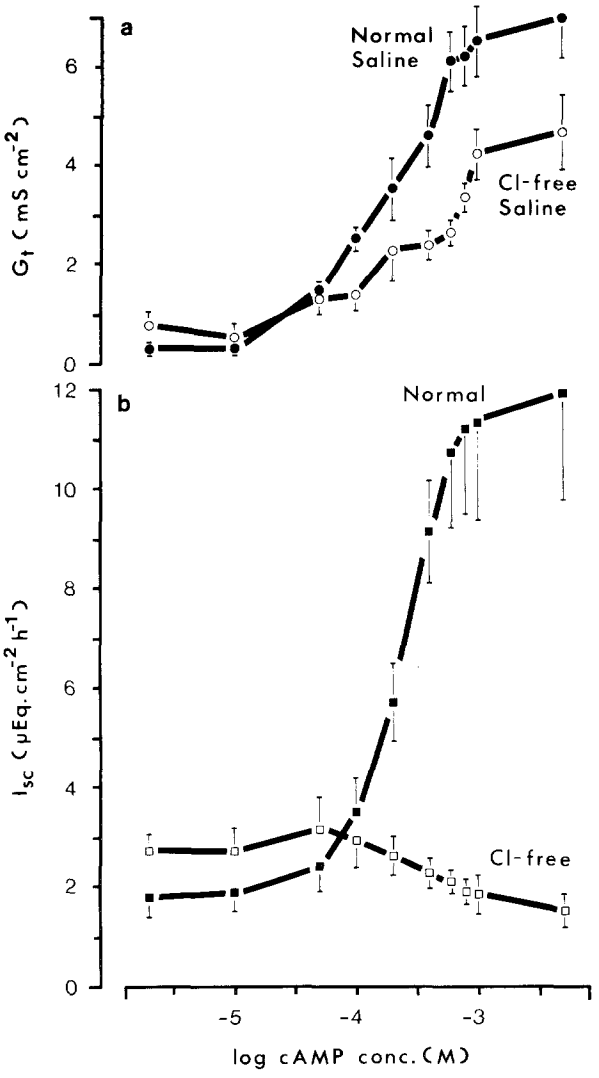


**Fig. 16.** Log dose-response curve showing the relationship between cAMP concentration and (*a*) transepithelial conductance ($G_t$), and (*b*) $I_{sc}$. Tissues were bathed in normal or Cl-free saline. Means ± SE; $n$ = 6 recta (normal saline), 4 recta (Cl-free saline)

## Localization of the Active Step

Chloride entry across the apical membrane occurs against a net electrochemical potential under both open- and short-circuit conditions while Cl flux across both membranes is in the mucosa-to-serosa direction, as demonstrated in the companion paper by measuring tracer fluxes under the same conditions. Although Cl entry into the rectal cell is active, the insensitivity of $J^{Cl}_{net}$ to a very large reduction in $\Delta\bar{\mu}^a_{Na}/F$ [23], and the lack of correlation between $\Delta\bar{\mu}^a_{Cl}/F$ and $\Delta\bar{\mu}^a_{Na}/F$ provides further evidence that Cl entry is not driven by NaCl cotransport across the apical membrane.

Cyclic-AMP (1 mM) and low levels of K stimulate both $J^{Cl}_{net}$ and the $\Delta\bar{\mu}^a_{Cl}/F$ opposing Cl entry across the apical membrane under steady-state $I_{sc}$ and open-circuit conditions. Also, small quantities of K stimulate $I_{sc}$ only when added to the mucosal side [19]. The effects of K (2 to 4 mM) on $\Delta\bar{\mu}^a_{Cl}/F$ cannot be explained by electrical coupling across the apical membrane or the entire rectal wall; K must stimulate the active mechanism in some manner. It is interesting that intracellular K activity is maintained near control levels (66.9 mM) when 10 mM K is present only on the serosal side of locust rectum. Since $J^{Cl}_{net}$ is not stimulated by K under these conditions [19], K apparently acts on Cl entry at an external site on the apical membrane.

Intracellular ion activities are determined by the properties of both apical and basal membranes. If the Cl conductance of the serosal border is much higher than that of the apical membrane, changes in $a^c_{Cl}$ will be affected by changes in $V_b$, even if $a^c_{Cl}$ is maintained above equilibrium by the action of an apical Cl pump. For example, short-circuiting hyperpolarizes $V_b$ and depolarizes $V_a$ by approximately equal amounts in locust rectum because the voltage divider ratio is near one. Since the partial ionic conductance of the basal membrane to Cl is higher than that of the apical membrane, more Cl would be driven out of the cell across the basal membrane by $I_{sc}$-induced hyperpolarization of $V_b$ than would be drawn into the cell by depolarization of $V_a$. Indeed, $a^c_{Cl}$ was higher under open-circuit conditions (46.2 ± 1.3 mM, 49 cells, 5 tissues) than under $I_{sc}$ conditions (40.3 ± 0.9 mM, 40 cells, 4 tissues; $P < 0.01$). We emphasize that this effect of $V_b$ on $a^c_{Cl}$ does not affect our conclusions regarding the location of the active step for Cl transport or the stimulatory effect of cAMP and K on the active process because they are based on comparisons of $\Delta\bar{\mu}^a_{Cl}$ and $J^{Cl}_{net}$ under the same steady-state conditions. Because the net flux of Cl across apical and basal membranes and the entire epithelium are equal at steady state, measurements of $J^{Cl}_{net}$ and $\Delta\bar{\mu}^a_{Cl}$ are sufficient to show that energy is required for Cl entry.

Changes in cell volume could also affect intracellular ion activities and calculated electrochemical gradients, but total tissue water, extracellular water and intracellular volume (nonmannitol space, NMS) were not different in controls and cAMP-treated tissues ($P \gg 0.2$). Therefore, the 50% increase in $a^c_{Cl}$ during exposure to cAMP cannot be attributed to cell shrinkage. That NMS provides a valid estimate of cell volume is suggested by i) the drastic decline in NMS during exposure to high osmotic pressure and ii) the fact that nonmannitol space agrees very well with our estimates of total

intracellular volume based on cell dimensions (3.61 ± 0.24 *vs.* 3.3 μl; [19]).

## Possible Sources of Energy for Cl Entry

Sodium entry across the apical membrane is strongly favored when the mucosal side is perfused with normal saline (115 mM [Na]; $\Delta\bar{\mu}^a_{Na}/F \simeq -122$ mV) and $\Delta\bar{\mu}^a_{Na}/F$ is more than adequate to drive Cl entry by NaCl cotransport ($\Delta\bar{\mu}^a_{Cl}/F = 45$ mV). However, no interdependence between $\Delta\bar{\mu}^a_{Na}/F$ and $J^{Cl}_{net}$ [23] or $\Delta\bar{\mu}^a_{Na}/F$ and $\Delta\bar{\mu}^a_{Cl}/F$ (Fig. 8) were observed and there is considerable evidence that Cl fluxes and Cl-dependent $I_{sc}$ are insensitive to Na removal [22]. Net Na fluxes across stimulated recta *in vivo* and *in vitro* are very low compared to $J^{Cl}_{net}$ and are insensitive to cAMP [43].

$\Delta\bar{\mu}^a_K$ is near 0 mV under $I_{sc}$ conditions; therefore a K-coupled influx could supply little if any energy for Cl transport across the apical membrane.

Most cells possess an inward-directed net electrochemical potential for protons of ~60 mV; however HCl cotransport or Cl/OH exchange seem unlikely to drive Cl transport across locust rectum because $I_{sc}$ is not affected by raising external pH from 6.2 to 8.0 [19, 21], a maneuver which should reverse or at least greatly diminish $\Delta\bar{\mu}^a_H$ if we may assume intracellular pH to be in the range (7.0 to 7.4) observed in other cells. Furthermore, reducing mucosal pH below 5.5 inhibits rather than stimulates $I_{sc}$ (half-maximal inhibition at approximately pH = 4.7), contrary to expectations with HCl coentry.

In short, we have been unable to find evidence that Cl absorption is secondarily active in locust rectum and the possibility of a Cl-ATPase pump should be seriously considered for this tissue. There are reports of anion-stimulated ATPases in recta of locusts [25] and dragonfly larvae [26] but it is uncertain whether this is localized in the plasma membrane.

## K and Na Electrochemical Potentials

Both apical and basal membrane K gradients are consistent with passive K movement in the mucosa-to-serosa direction. A small $J^K_{net}$ has been observed during cAMP stimulation in short-circuited recta; however, the electrochemical potentials are too small to permit localization of the active step for transepithelial K transport with certainty. Regardless, we have found that this active absorption is quantitatively much less important: passive K reabsorption under normal open-circuit conditions constitutes ~85% of net K flux and is electrically coupled to Cl transport [23].

There is active Na absorption across locust rectum under these $I_{sc}$ conditions (1 μeq $cm^{-2}hr^{-1}$; K. Black, *unpublished observation*); however, the rate is much lower than that of Cl (about 10 μeq $cm^{-2}hr^{-1}$ during cAMP exposure) and it does not contribute significantly to $I_{sc}$. The present results suggest that, like epithelia in vertebrates, Na entry across the apical membrane is favored by a large net electrochemical gradient of 120 mV when Na-rich saline is present bilaterally. Also, ion-sensitive microelectrode data are consistent with an active step at the basal membrane since any Na entering the cells from the mucosal side would have to be pumped across the basal cell border against a $\Delta\bar{\mu}^b_{Na}/F$ of 120 mV.

## Locust Rectum is a Tight Epithelium having Low Electrical Resistance

Results from several techniques indicate that locust rectum is a tight epithelium: 1) Deflections in $V_t$ produced by transepithelial salt gradients were strongly dependent on the direction of the gradient, indicative of two barriers in series having different properties. Such asymmetry would not be expected if ion diffusion occurred through a single paracellular barrier, since tight junctions in other tissues are not known to rectify. 2) Voltage scanning did not reveal any low-resistance regions. This technique is qualitative in nature and there is the possibility that small leaks could go undetected, but in this connection, negative results have been reported for other tight epithelia whereas paracellular shunting has been detected by voltage scanning *Necturus* gallbladder [13] and MDCK cultures [8]. 3) Cable analysis of the epithelium indicates that locust rectum is moderately tight under control conditions, when 60% of $G_t$ is transcellular, and becomes functionally tighter during cAMP stimulation, when transcellular conductance ranges between 89 and 96% of the total. The fractional conductance of the transcellular pathway of locust rectum under these conditions is similar to that of other tight epithelia (53%, toad bladder [36]; 80%, *Necturus* stomach [42]; 65 to 96%, rabbit urinary bladder [28]; 31%, rabbit cornea [30]), but is much higher than that of leaky epithelia (~4% *Necturus* gallbladder [13], *Necturus* proximal tubule [17]). Locust rectum is tight because the cell membrane resistances per macroscopic area are extremely low, and in this respect resembles vertebrate salivary duct [1] and gastric mucosa [9].

Many insect epithelia are probably tight, although this has not previously been directly shown.

For example, Berridge et al. [4] demonstrated that $R_t$ of blowfly salivary gland falls from 80 Ω cm$^2$ at rest to 5.5 Ω cm$^2$ during stimulation with 5-HT. This large decline and the small effect of 5-HT on $V_b$ argue against a large paracellular shunt in blowfly salivary gland. Malpighian tubules and lepidopteran midgut also maintain large chemical and electrical gradients while having low electrical resistance (ca. 40 Ω cm$^2$, [49], and ~150 Ω cm$^2$, [50], respectively).

## Regulation of Passive Permeability by cAMP

Addition of cAMP, cGMP or theophylline stimulates $I_{sc}$ (1000%) and $G_t$ (50 to 60%; [19]). When the voltage deflections across apical and basal membranes during transepithelial current pulses are monitored before and after cAMP addition, both apical and basal voltage deflections are greatly reduced, suggesting a decline in apical and basal membrane resistances. This was confirmed and quantified by measuring the radial spread of intracellularly injected current. Since $\Delta G_b$ was nearly abolished in Cl-free saline whereas $\Delta R_a$ was K-dependent, the simplest explanation for these observations is that cAMP increases apical membrane conductance to K by ~18 mS cm$^{-2}$, and increases basal membrane Cl conductance by approximately ~19 mS cm$^{-2}$. It is clear from Fig. 16 that both processes have similar cAMP dose-response curves and might be turned on simultaneously by a CTSH-induced rise in intracellular cAMP. The large increase in apical membrane K conductance observed in this study would explain the 400% stimulation $J^K_{sm}$ by cAMP seen previously by measuring $^{42}$K fluxes. The $R_a$ calculated under KCl-free conditions is lower than estimated when the saline is only Cl-free. Our explanation for this paradox is that $R_a$ and $\alpha$ are underestimated in KCl-free saline because $V_a$ does not reach a steady-state value during 1-sec current pulses. The transient response of $\Delta V_a$ to current pulses could not be attributed to capacitance since apical membrane area would have to be 50,000 times greater than the macroscopic tissue area (assuming 1 μF cm$^{-2}$) in order to explain the observed time constant. A more detailed analysis will be required to determine whether the transient is due to membrane polarization-transport number effects, voltage-dependent conductance, or some other mechanism [37]. At present the important finding is that K-removal blocks $\Delta G_a$ during cAMP exposure.

Addition of cAMP stimulates net Cl flux by approximately 4 to 5 μeq cm$^{-2}$hr$^{-1}$ under open-circuit conditions while the net electrochemical gradient favoring Cl exit across the basal membrane $\Delta\bar{\mu}^b_{Cl}$ is ~20 mV. Converting net Cl flux to current, 5 μeq cm$^{-2}$hr$^{-1}$ becomes 134 μA cm$^{-2}$, and the minimum increase in basal membrane chord conductance required for Cl efflux by electrodiffusion would be (134.1 × 10$^{-6}$ A cm$^{-2}$)/(20 × 10$^{-3}$ V) = 6.7 mS cm$^{-2}$ or only 30% of the $\Delta G_b$ during cAMP stimulation. The increase in $G_b$ is approximately twice that required for passive exit, even after subtracting the possible error caused by interfering anions on $a^c_{Cl}$ (4.9 mM) and allowing for a 36% higher rate of Cl transport during the present experiments as suggested by the low values of $R_t$ shown in Table 3. Some uncertainty results from the use of different tissues for flux, ion sensitive microelectrode, and cable analysis experiments, and from the small sample size in the latter. Another possible source of error might be our neglect of distributed current flow at the lateral border, although as noted above, these should be small. Recent current fluctuation analyses [24] indicate that the basal membrane has substantial numbers of Ba-blockable K channels.

## Equivalent Electrical Circuit Parameters

When the apical and basal membranes and tight junctions are replaced with Thevenin equivalents (Fig. 1*a*), $V_a$, $V_b$ and $V_t$ are given by

$$V_a = [E_a(R_b + R_j) + R_a(E_b + E_j)]/(R_a + R_b + R_j) \quad (9)$$

$$V_b = [E_b(R_a + R_j) + R_b(E_a + E_j)]/(R_a + R_b + R_j) \quad (10)$$

$$V_t = (V_a - V_b)R_j/(R_a + R_b + R_j) \quad (11)$$

when $V_a$, $E_a$, $V_b$ and $E_b$ are measured with respect to the intracellular compartment, and $V_t$ and $E_j$ to the serosal side. With these polarities, the equivalent electromotive force across apical ($E_a$) and basal ($E_b$) membranes are

$$E_a = V_a - V_t R_a/R_j \quad (12)$$

$$E_b = V_b + V_t R_b/R_j \quad (13)$$

if we assume that $E_j = 0$ when identical solutions are used on both sides of the epithelium. A small $E_j$ would exist if ions were more concentrated in the intercellular spaces and there is evidence for elevated [K] in the lateral spaces of insect recta (reviewed in [23]). However, our results were obtained *in vitro* using vigorously perfused tissues which had been exposed to isosmotic saline for many hours. These conditions would be expected to dissipate any gradients that might be present *in vivo*. Also, we observed no unusually high ion activities with ion-sensitive microelectrodes although we would

**Table 5.** Calculation of steady-state equivalent electromotive forces ($E_a$ and $E_b$, respectively) across apical and basal membranes

| Saline | $V_a$[a] | $V_b$ | $V_t$ | $R_a/R_j$ | $R_b/R_j$ | $E_a$ | $E_b$ |
|---|---|---|---|---|---|---|---|
| | | (mV) | | | | (mV) | |
| Control | 57.8 | 50.6 | 7.2 | 0.2965 | 0.2605 | 55.7 | 52.5 |
| +cAMP | 70.2 | 38.0 | 32.2 | 0.0711 | 0.0581 | 67.9 | 39.9 |
| Cl-free[b] | 56.7 | 50.4 | 6.3 | 0.0633 | 0.4100 | 56.3 | 53.0 |

[a] Voltages from Table 2 and unpublished observations.
[b] Recta were bathed in nominally Cl-free saline in which Cl was replaced by gluconate. $V_a$ and $V_b$ are with respect to the intracellular compartment; $V_t$ is with respect to the serosal side.

have expected to impale hypertonic lateral spaces occasionally despite their small size (<5 $\mu$m).

Table 5 shows the equivalent emf's calculated for apical and basal membranes of unstimulated recta in normal saline (control) during exposure to 1 mM cAMP, and during cAMP-stimulation in Cl-free saline. Membrane and junctional resistances were taken from Table 4 and Table 5 to calculate $R_{a,b}/R_j$. The Table clarifies several points: i) addition of 1 mM cAMP increased $E_a$ by 12 mV as would be expected if an absorptive Cl pump at the apical membrane were stimulated. Also, removing Cl from cAMP-stimulated recta returned $E_a$ to the control value. ii) In normal saline, exposure to cAMP resulted in a decline in $E_b$, consistent with enhanced Cl exit out of the cells across the basal membrane. This $\Delta E_b$ can be explained by a large increase in Cl conductance because intracellular Cl is above electrochemical equilibrium across the basal membrane, and $\Delta E_b$ is nearly identical to the net electrochemical potential favoring Cl exit ($\Delta\bar{\mu}^b_{Cl}/F$ = 23.3 ± 1.4 mV).

## A Cellular Model for KCl Absorption across Locust Rectum

Figure 17 summarizes previous tracer flux results and the main conclusions of this paper. Transepithelial absorption requires active Cl entry across the apical membrane, and this process is apparently electrogenic and is stimulated by cAMP and mucosal K ions. Although the mechanism by which K stimulates Cl entry is not firmly established, it apparently does not involve a KCl cotransport step at the apical membrane, because i) transepithelial K fluxes are insensitive to Cl removal [19], ii) the apical membrane hyperpolarizes during cAMP exposure after equilibration in K-free saline (consistent with electrogenic Cl entry under these

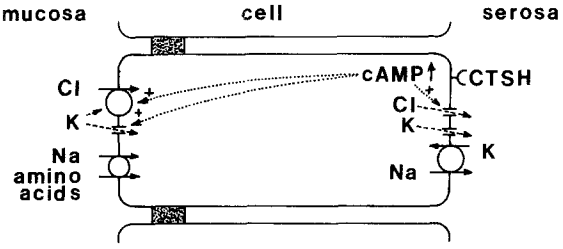


**Fig. 17.** Summary diagram of the cellular mechanism and regulation of KCl transport across locust rectum. Cl enters the cell across the apical membrane by an active mechanism which is thought to be electrogenic and K-stimulated; potassium enters through a parallel conductive pathway. Cl exits across the basal membrane via a conductive pathway, and most K probably leaves the cell by electrodiffusion. The peptide hormone CTSH (chloride transport stimulating hormone) elevates intracellular cAMP [35], which stimulates active Cl entry, apical membrane K conductance, and basal membrane Cl conductance

conditions), and iii) 35% of the cAMP-stimulated $I_{sc}$ is K-independent. Another important effect of cAMP is to reduce transepithelial resistance by ~50%, through increases in the conductance of both cell membranes. The stimulation of apical membrane conductance is K-dependent whereas the increase in basal membrane conductance is Cl-dependent. Regulation of KCl by the peptide hormone CTSH would be unusually efficient because both electrogenic Cl transport and counter-ion permeability are stimulated by cAMP ($J^K_{net}$ exactly matches $J^{Cl}_{net}$ under open-circuit conditions [23]). In addition to on/off hormonal control mediated by cAMP, mucosal [K] also modulates the rate of KCl absorption by enhancing active Cl transport at low mucosal K levels and by inhibiting active Cl transport and passive K permeability at high concentrations [23].

We thank Drs. W. Prince, N. Wills, J. Steeves and S. Lewis for instruction in microelectrode methods, and D. Jenkins of Dow Corning, Vancouver, for the gift of 1107 silicon oil. NSERC (Canada) provided a graduate scholarship to J.W.H. and operating grants to J.E.P.

## References

1. Augustus, J., Bijman, J., Os, C.H. van 1978. Electrical resistance of rabbit submaxillary main duct: A tight epithelium with leaky cell membranes. *J. Membrane Biol.* **43**:203–226
2. Baumgarten, C.M., Fozzard, H.A. 1981. Intracellular chloride activity in mammalian ventricular muscle. *Am. J. Physiol.* **241**:C121–C129
3. Berridge, M.J. 1981. Hormone-induced changes in ion level during stimulation of fluid secretion by gland cells. *In:* The Application of Ion-selective Microelectrodes. T. Zeuthen, editor. pp. 61–74. North-Holland Biomedical, New York

4. Berridge, M.J., Lindley, B.D., Prince, W.T. 1975. Membrane permeability changes during stimulation of isolated salivary glands of *Calliphora* by 5-hydroxytryptamine. *J. Physiol. (London)* **244:**549–567
5. Berridge, M.J., Schlue, W.R. 1978. Ion-selective electrode studies on the effects of 5-hydroxytryptamine on the intracellular level of potassium in an insect salivary gland. *J. Exp. Biol.* **72:**203–216
6. Blankemeyer, J.T., Duncan, R.L. 1980. The potassium activity in a polymorphic potassium active transporting epithelium, insect midgut. *Fed. Proc.* **39:**1711
7. Boulpaep, E.L., Sackin, H. 1980. Electrical analysis of intraepithelial barriers. *In:* Current Topics in Membranes and Transport. F. Bronner and A. Kleinzeller, editors. Vol. 13, pp. 169–197. Academic, New York
8. Cereijido, M., Borboa, L., Gonzalez-Mariscal, L. 1983. Occluding junctions and paracellular pathway in monolayers of MDCK cells. *J. Exp. Biol.* **106:**205–215
9. Clausen, C., Machen, T.E., Diamond, J. 1983. Use of AC impedance analysis to study membrane changes related to acid secretion in amphibian gastric mucosa. *Biophys. J.* **41:**167–178
10. Delong, J., Civan, M.M. 1978. Dissociation of cellular $K^+$ accumulation from net $Na^+$ transport by toad urinary bladder. *J. Membrane Biol.* **42:**19–43
11. Duffey, M.E., Turnheim, K., Frizzell, R.A., Schultz, S.G. 1978. Intracellular chloride activities in rabbit gallbladder: Direct evidence for the role of the sodium-gradient in energizing "uphill" chloride transport. *J. Membrane Biol.* **42:**229–245
12. Eisenberg, R.S., Johnson, E.A. 1970. Three-dimensional electrical field problems in physiology. *In:* Progress in biophysics and molecular biology. J.A.V. Butler and D. Noble, editors. Vol. 20, pp. 1–65. Pergamon, Toronto
13. Frömter, E. 1972. The route of passive ion movement through the epithelium of *Necturus* gallbladder. *J. Membrane Biol.* **8:**259–301
14. Fujimoto, M., Kotera, K., Matsumura, Y. 1980. The direct measurement of K, Cl, Na and H ions in bullfrog tubule cells. *In:* Current Topics in Membranes and Transport. F. Bronner and A. Kleinzeller, editors. Vol. 13, pp. 49–61. Academic, New York
15. Fujimoto, M., Kubota, T. 1976. Physicochemical properties of a liquid ion exchanger microelectrode and its application to biological fluid. *Jpn. J. Physiol.* **26:**631–650
16. Greger, R. 1981. Chloride reabsorption in the rabbit cortical thick ascending limb of Henle's loop of rabbit kidney. *Pfluegers Arch.* **390:**30–37
17. Guggino, W.B., Windhager, E.E., Boulpaep, E.L., Giebisch, G. 1982. Cellular and paracellular resistances of the *Necturus* proximal tubule. *J. Membrane Biol.* **67:**143–154
18. Gupta, B.L., Wall, B.J., Oschman, J.L., Hall, T.A. 1980. Direct microprobe evidence of local concentration gradients and recycling of electrolytes during fluid absorption in the rectal papillae of *Calliphora*. *J. Exp. Biol.* **88:**21–47
19. Hanrahan, J.W. 1982. Cellular mechanism and regulation of KCl transport across an insect epithelium. Ph.D. Thesis. University of British Columbia, Vancouver
20. Hanrahan, J.W., Meredith, J., Phillips, J.E., Brandys, D. 1983. Methods for the study of transport and control in insect hindgut. *In:* Measurement of Ion Transport and Metabolic Rate in Insects. T. Bradley and T. Miller, editors. pp. 19–67. Springer-Verlag, New York
21. Hanrahan, J.W., Phillips, J.E. 1982. Electrogenic, $K^+$-dependent chloride transport in locust hindgut. *Philos. Trans. R. Soc. London B* **299:**585–595
22. Hanrahan, J.W., Phillips, J.E. 1982. K and cAMP stimulate the Cl pump in locust rectum. *Am. Zool.* **22:**914
23. Hanrahan, J.W., Phillips, J.E. 1983. Mechanism and control of salt absorption in locust rectum. *Am J. Physiol.* **224:**R131–R142
24. Hanrahan, J.W., Wills, N.K., Lewis, S.A. 1983. Barium-induced current fluctuations from the basal membrane of an insect epithelium. *Proc. Int. Congr. Physiol. Sci.* p. 457
25. Herrera, L., Lopes-Moratalla, N., Santiago, E., Ponz, F., Jordana, R. 1978. Effect of bicarbonate on chloride-dependent transmural potential and ATPase activity in the rectal wall of *Schistocerca gregaria*. *Rev. Esp. Fisiol.* **34:**219–224
26. Komnick, H., Schmitz, M.H., Hinssen, H. 1980. Biochemischer Nachweis von $HCO_3^-$- und $Cl^-$-abhängigen ATPase-activitäten im rectum von anisopteranen Libellenlarven und Hemmung der rectalen Chloridaufnahme durch thiocyanat. *Eur. J. Cell. Biol.* **20:**217–227
27. Kotera, K., Satake, N., Honda, M., Fujimoto, M. 1979. The measurement of intracellular sodium activities in the bullfrog by means of a double-barrelled sodium ion-exchange microelectrode. *Membr. Biochem.* **2:**323–338
28. Lewis, S.A., Eaton, D.C., Diamond, J.M. 1976. The mechanism of $Na^+$ transport by rabbit urinary bladder. *J. Membrane Biol.* **28:**41–70
29. Loewenstein, W.R. 1981. Junctional intercellular communication: The cell-to-cell membrane channel. *Physiol. Rev.* **61:**829–913
30. Marshall, W.S., Klyce, S.D. 1983. Cellular and paracellular pathway resistances in the "tight" $Cl^-$-secreting epithelium of rabbit cornea. *J. Membrane Biol.* **73:**275–282
31. Moffett, D.F., Hudson, R.L., Moffett, S.B., Ridgway, R.L. 1982. Intracellular $K^+$ activities and cell membrane potentials in a $K^+$-transporting epithelium, the midgut of tobacco hornworm (*Manduca sexta*). *J. Membrane Biol.* **70:**59–68
32. Ogden, T.E., Citron, M.C., Pierantoni, R. 1978. The jet stream microbeveler: An inexpensive way to bevel ultrafine glass micropipettes. *Science* **201:**469–470
33. Olver, F.W.J. 1967. Bessel functions of integer order. *In:* Handbook of Mathematical Functions. M. Abramowitz and J.A. Stegun, editors. pp. 355–422. National Bureau of Standards, Washington, D.C.
34. Phillips, J.E. 1964. Rectal absorption in the desert locust *Schistocerca gregaria* Forskål. II. Sodium, potassium and chloride. *J. Exp. Biol.* **41:**39–67
35. Phillips, J. 1970. Apparent transport of water by insect excretory systems. *Am. Zool.* **10:**413–436
36. Reuss, L., Finn, A.L. 1974. Passive electrical properties of toad urinary bladder epithelium. Intercellular electrical coupling and transepithelial cellular and shunt conductances. *J. Gen. Physiol.* **64:**1–25
37. Reuss, L., Finn, A.L. 1977. Mechanisms of voltage transients during current clamp in *Necturus* gallbladder. *J. Membrane Biol.* **37:**299–319
38. Reuss, L., Weinman, S.A. 1979. Intracellular ionic activities and transmembrane electrochemical potential differences in gallbladder epithelium. *J. Membrane Biol.* **49:**345–362
39. Robinson, R.A., Stokes, R.H. 1970. Electrolyte solutions (2nd ed., revised). Butterworths, London
40. Shiba, H. 1971. Heaviside's "Bessel cable" as an electric model for flat simple epithelial cells with low resistive junctional membranes. *J. Theor. Biol.* **30:**59–68

41. Socolar, S.J., Politoff, A.L. 1971. Uncoupling cell junctions of a glandular epithelium by depolarizing current. *Science* **172:**492–494
42. Spenney, J.G., Shoemaker, R.L., Sachs, G. 1974. Microelectrode studies of fundic gastric mucosa: Cellular coupling and shunt conductance. *J. Membrane Biol.* **19:**105–128
43. Spring, J.H., Phillips, J.E. 1980. Studies on locust rectum: II. Identification of specific ion transport processes regulated by corpora cardiacum and cyclic-AMP. *J. Exp. Biol.* **86:**225–236
44. Spring, K.R., Kimura, G. 1978. Chloride reabsorption by renal proximal tubules of *Necturus*. *J. Membrane Biol.* **38:**233–254
45. Stewart, W.W. 1978. Functional connections between cells as revealed by dye-coupling with a highly fluorescent naphthalimide tracer. *Cell* **14:**741–759
46. Vietinghoff, U.E., Olszewska, E., Janiszewski, L. 1969. Measurement of the biolectric potentials in the rectum of *Locusta migratoria* and *Carausius morosus* in *in vitro* preparations. *J. Insect Physiol.* **15:**1273–1277
47. Walker, J.L. 1971. Ion specific liquid ion exchanger microelectrodes. *Anal. Chem.* **43:**89A–92A
48. Williams, D., Phillips, J., Prince, W., Meredith, J. 1978. The source of short-circuit current across locust rectum. *J. Exp. Biol.* **77:**107–122
49. Williams, J.C., Jr. 1983. The Malpighian tubule of the yellow fever mosquito: Its function *in vitro* and *in vivo*. Ph.D. Thesis. Cornell University, Ithaca
50. Wood, J.L., Moreton, R.B. 1978. Refinements in the short-circuit technique, and its application to active potassium transport across the *Cecropia* midgut. *J. Exp. Biol.* **77:**123–140

Received 16 December 1983